WPJET4 Gamma Camera Upgrade (GCU)

Additional report	Tests of upgraded Gamma Camera in the final installation position at JET

1. Introduction

After the installation of all 19 detectors, in March and May 2017, in the horizontal and vertical parts of the Gamma Camera (GC), it was necessary to conduct tests in the final position inside the Torus Hall at JET. The energy calibration could be obtained with the use of radiation sources and the internal activity of lanthanum which contains a radioactive isotope ^{138}La.

The schedule of tests:

- 15th January 2018: Connection and signal check;
- 16th January 2018: Measurements performed with CAEN acquisition;
- 17th January 2018: Measurements performed with IST acquisition;
- 18th January 2018: Measurements performed with both acquisition and ^{137}Cs, ^{133}Ba sources.
- 22nd, 23rd and 24th January 2018: Measurements performed with both acquisition and ^{137}Cs, ^{133}Ba sources - finding an optimal operational voltage for each detector in GC.
- 25th and 26th January 2018: Measurements performed with both acquisition and ^{137}Cs, ^{133}Ba sources - finding an optimal operational voltage for each detector in GC, final tests.

2. Signal tests

Two devices installed at JET (FilterBox@NCBJ and MTCD@NCBJ) were turned on and the power voltage of each detector was set to a value V = 54.6 V. Due to an internal activity of $LaBr_3$, a signal is seen on the oscilloscope, checked for each detector. Waveforms are shown in Fig. 1.

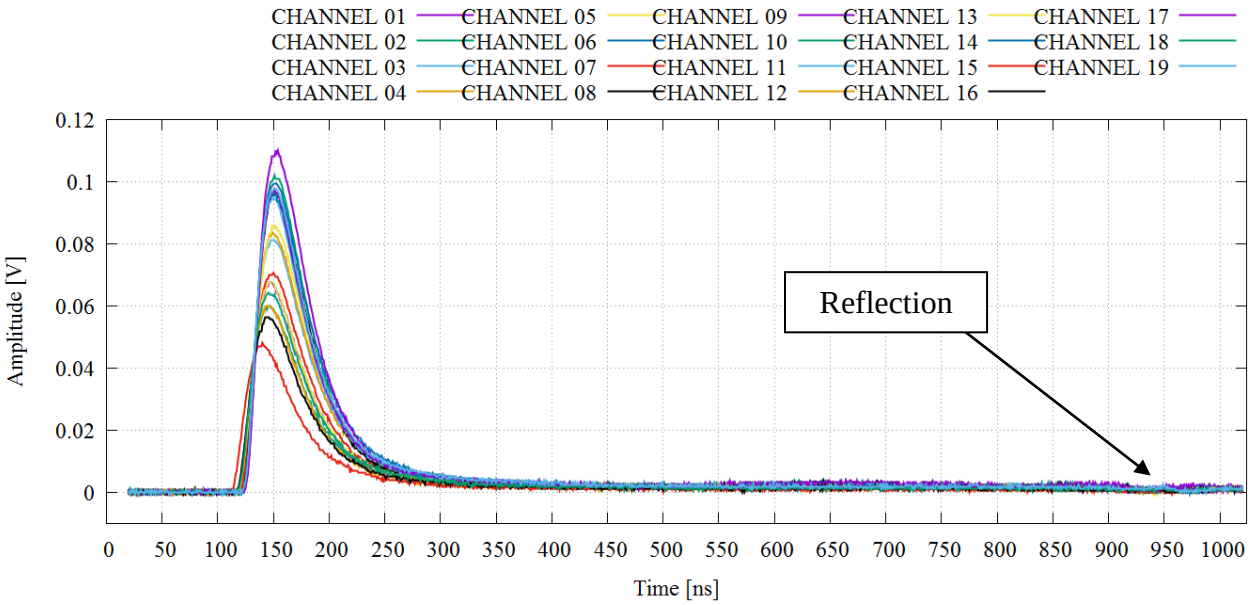

Fig. 1. Signals from 19 detectors installed in the Gamma Camera.

Time of each signal is about 100 ns and amplitude ≈40 mV which is consistent with previous results, presented in D20 “Report on M25: Detector assembly and laboratory tests with radioactive source and C&M”. A very low reflected signal can be seen about 800 ns after the original signal.

3. Measurements with CAEN acquisition

Test specification:
date: 16th January 2018,
voltage: 54.6 V at 20 °C for each detector,
time: 3600 s,
source: a weak ^{22}Na source placed at Gamma Camera,
data acquisition system: CAEN DT5730.

We used 6 channels in a CAEN device, so we divided a measurement into four parts: 5 detectors were working and one of them (in the channel #11) was used as a reference detector. The rate registered in this channel was about ≈13 cps.

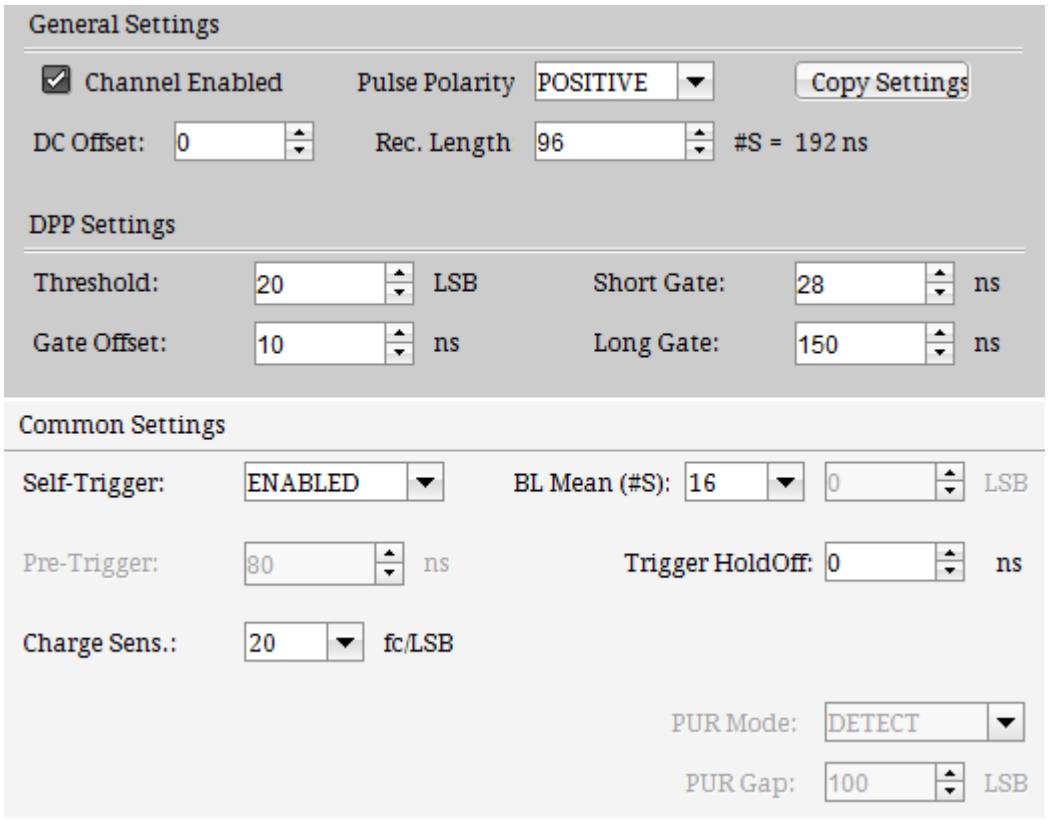

Fig. 2. Setting of the CAEN data acquisition system. All values were the same for each detector.

Table 1. Plan of measurements

No.	GC Channels	GC Reference channel	Source position	Comment
1	01, 02, 03, 04, 05	06	far	-
2	06, 07, 08, 09, 10	11	far	-
3	06, 07, 08, 09, 10	11	close	-
4	11, 12, 13, 14, 15	16	close	-
5	16, 17, 18, 19, 01	11	close	-
6	01, 02, 03, 04, 05	11	close	-

4. Spectra and peak identification

The source ^{22}Na emits two gamma lines: 511 keV and 1274 keV with the intensity 180.76% and 99.94%, respectively. The natural abundance of an isotope ^{138}La is a reason for an internal activity of $LaBr_3$. Gamma lines 789 keV and 1435 keV are emitted but peaks on the energy spectrum are not easily distinguishable. It is caused by X-rays emitted in coincidence with gamma lines, so on the spectra two characteristic regions are seen: a wide hump (789 keV) and a double peak coupled of 1435 keV and 1472 keV ["Development of MPPC-based detectors for high count rate DT campaigns at JET"].

The second peak of sodium is raising on the Compton edge of 1435 keV, which is about 1218 keV. Nevertheless, this peak could be useful to calibrate the energy spectrum but the Fermi function is needed to model a background. In May 2017 the measurement of a background was performed.

Three peaks were used to obtain the energy calibration with different fitting models:

- 511 keV: a single gauss and polynomial of 2nd order;
- 1274 keV: a single gauss and Fermi function;
- 1470 keV: a single gauss and polynomial of 2nd order.

Table 2. Results of the measurements

Channel No.	Peak position			FWHM at 511 keV [%]	Peak area			Rate [cps]
	511 keV	1274 keV	1470 keV		511 keV	1274 keV	1470 keV	
01	68	163	183	6.06	911	133	843	12.1
02	108	256	286	6.10	963	166	680	15.8
03	111	261	294	5.80	1269	159	728	16.2
04	67	160	181	5.21	1303	194	826	13.6
05	124	288	324	4.85	4336	228	752	18.9
06	89	210	237	5.70	1420	184	778	14.9
07	76	179	204	5.84	1177	394	794	14.2
08	110	260	291	6.13	1348	133	765	17.4
09	120	282	317	5.66	953	178	692	17.9
10	77	181	206	5.81	876	213	723	11.9
11	76	180	202	5.33	1106	255	768	12.3
12	76	180	203	6.25	1195	193	786	13.3
13	73	173	196	6.26	1272	248	800	13.3
14	80	191	215	5.92	1357	259	818	14.4
15	83	195	221	5.49	1405	276	817	14.8
16	78	185	209	5.35	1602	327	805	15.1

5. Measurements with ^{137}Cs, ^{22}Na sources

Test specification:

date: 18th, 19th January 2018,
voltage: 54.6 V at 20 °C for each detector,
time: 3600 s,
sources: ^{137}Cs and a weak ^{22}Na source placed at Gamma Camera,
data acquisition system: CAEN DT5730.

We used 6 channels in CAEN device, so we divide a measurement into four parts: 5 detectors were worked and one of them (in the channel #11) was used as a reference detector.

Setting of a CAEN data acquisition system was the same as in the previous measurements, see Fig. 2.

Table 3. Plan of measurements

No.	GC Channels	GC Reference channel	Source position	Comment
1	01, 02, 03, 04, 05	11	near	18th January
2	06, 07, 08, 09, 10	11	near	18th January
3	11, 12, 13, 14, 15	16	near	19th January
4	16, 17, 18, 19, 08	11	near	19th January

All spectra were compressed 16 times for analysis. Four peaks were used to obtain the linear energy calibration: 511 keV and 1274 keV from ^{22}Na, 662 keV from ^{137}Cs and 1470 keV from ^{138}La.

In Figs. 3-21 spectra collected for all 19 detectors are shown. Spectra with the ^{22}Na source are marked in purple, spectra with ^{133}Ba and ^{137}Cs sources are marked in green.

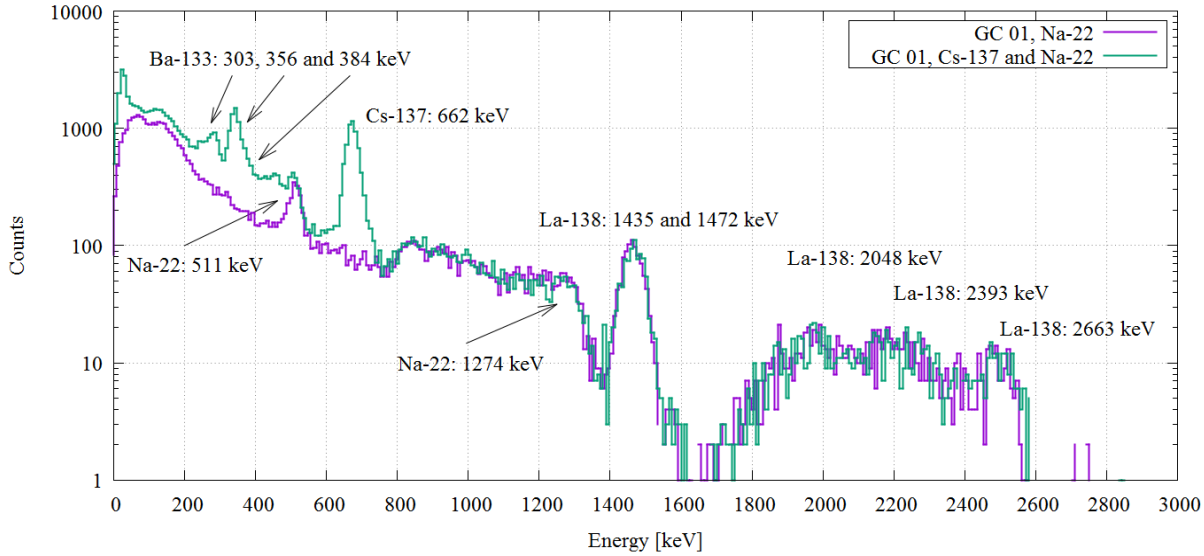

Fig 3. Gamma energy spectra of the GC 01.

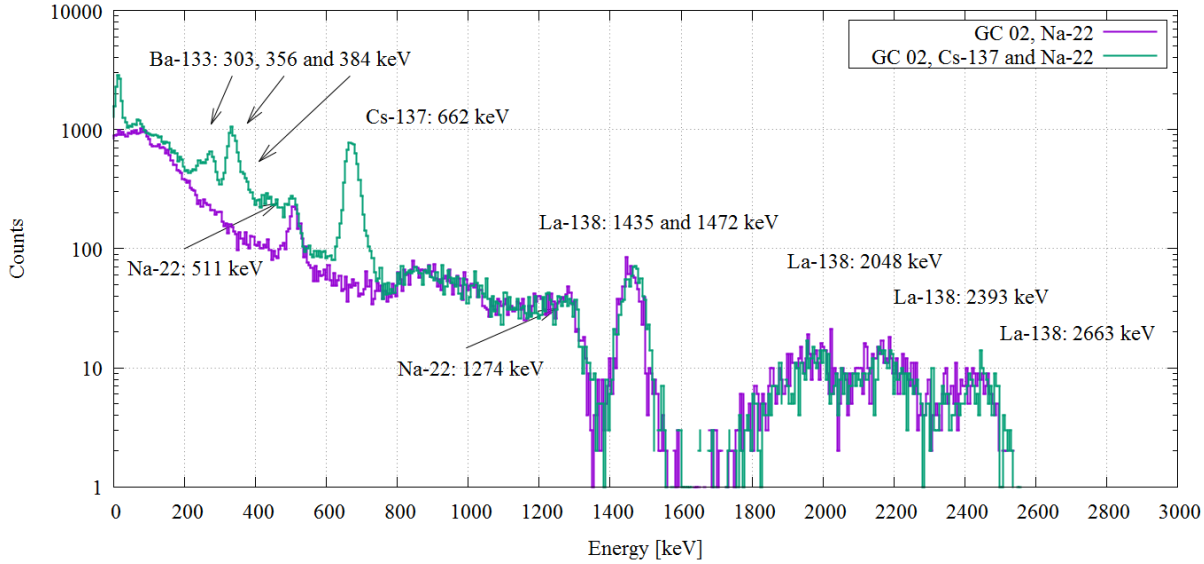

Fig 4. Gamma energy spectra of the GC 02.

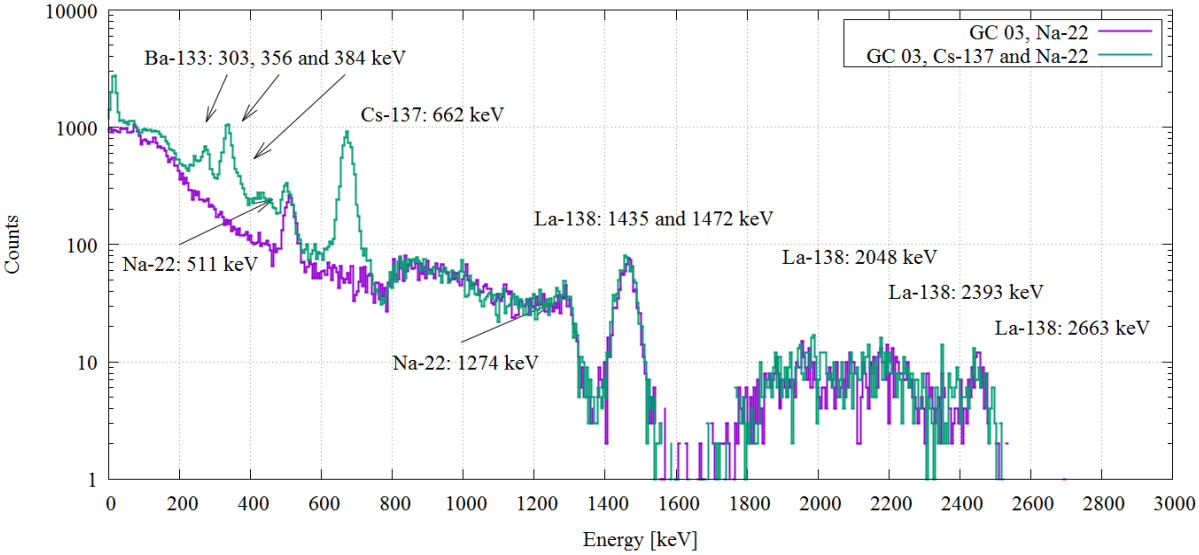

Fig 5. Gamma energy spectra of the GC 03.

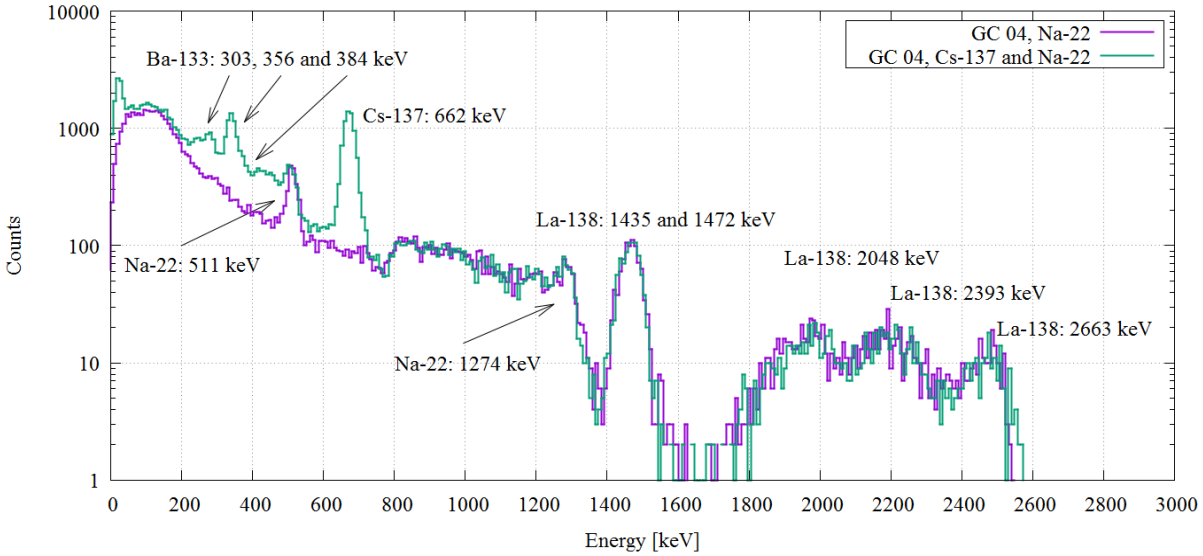

Fig 6. Gamma energy spectra of the GC 04.

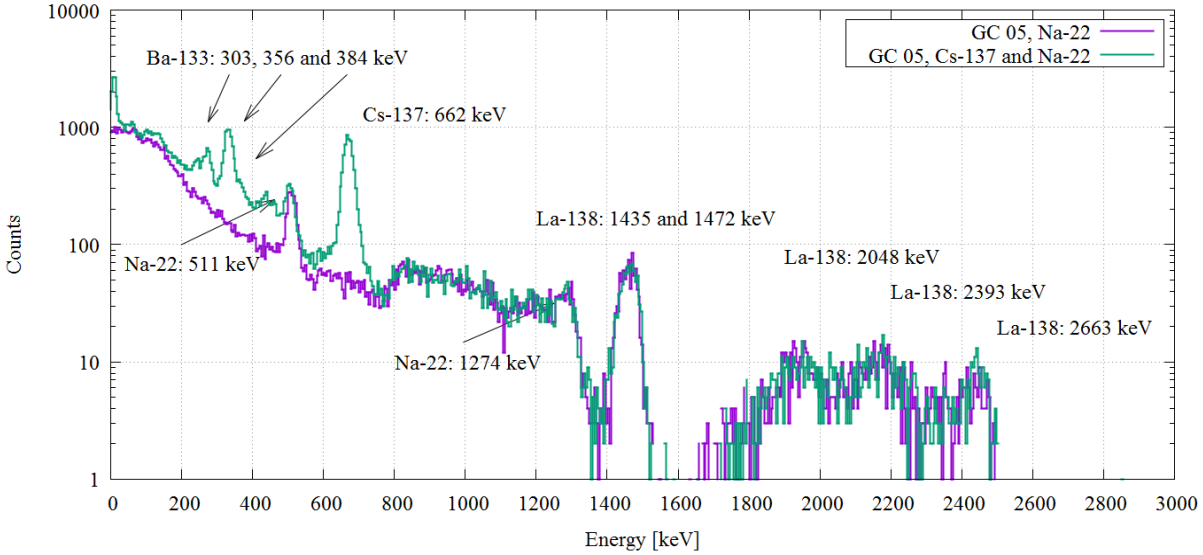

Fig 7. Gamma energy spectra of the GC 05.

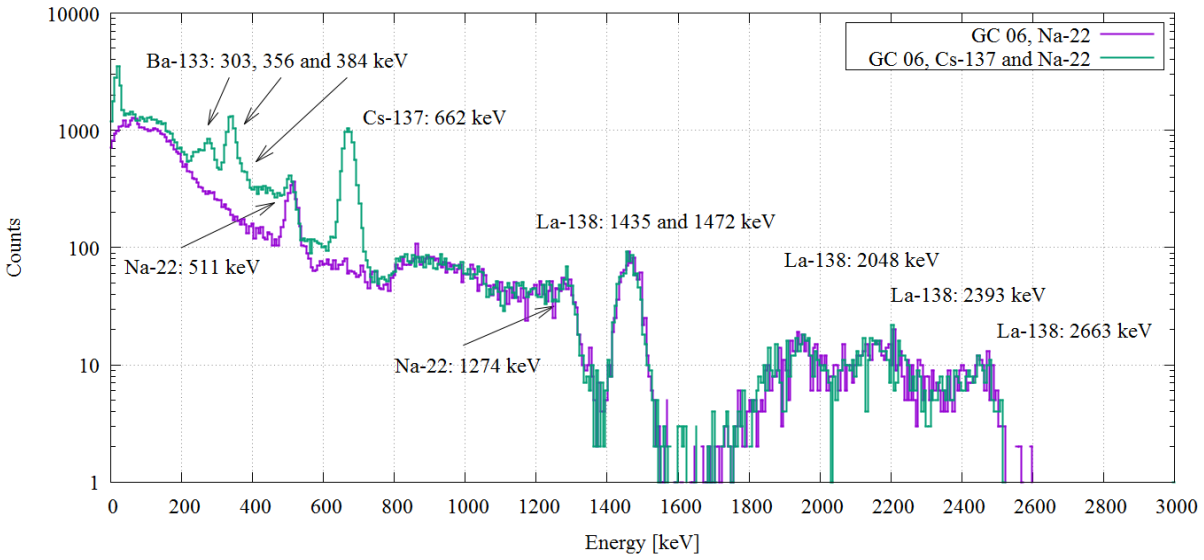

Fig 8. Gamma energy spectra of the GC 06.

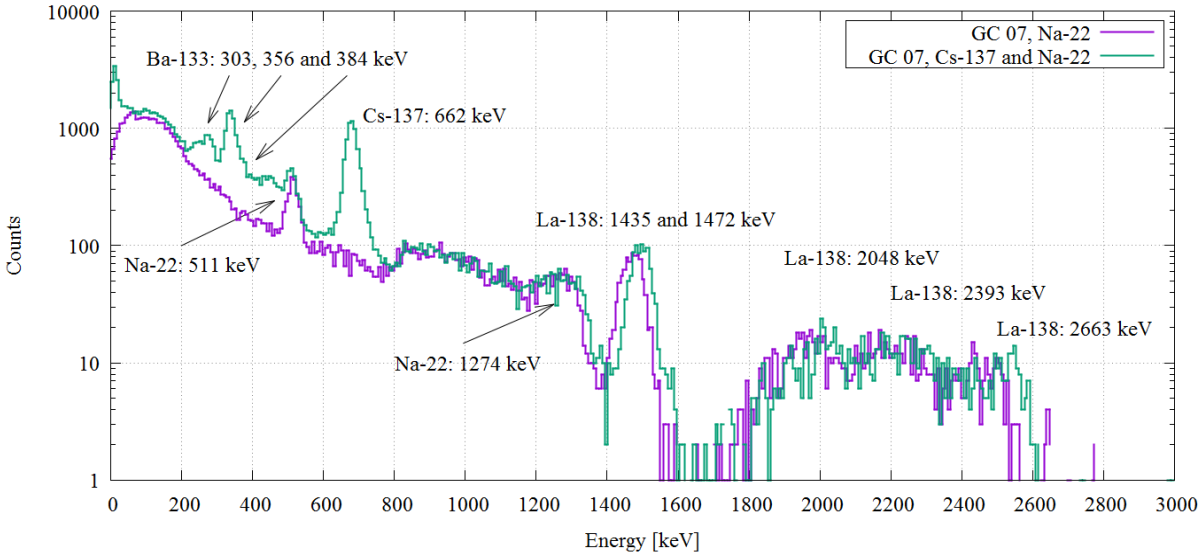

Fig 9. Gamma energy spectra of the GC 07.

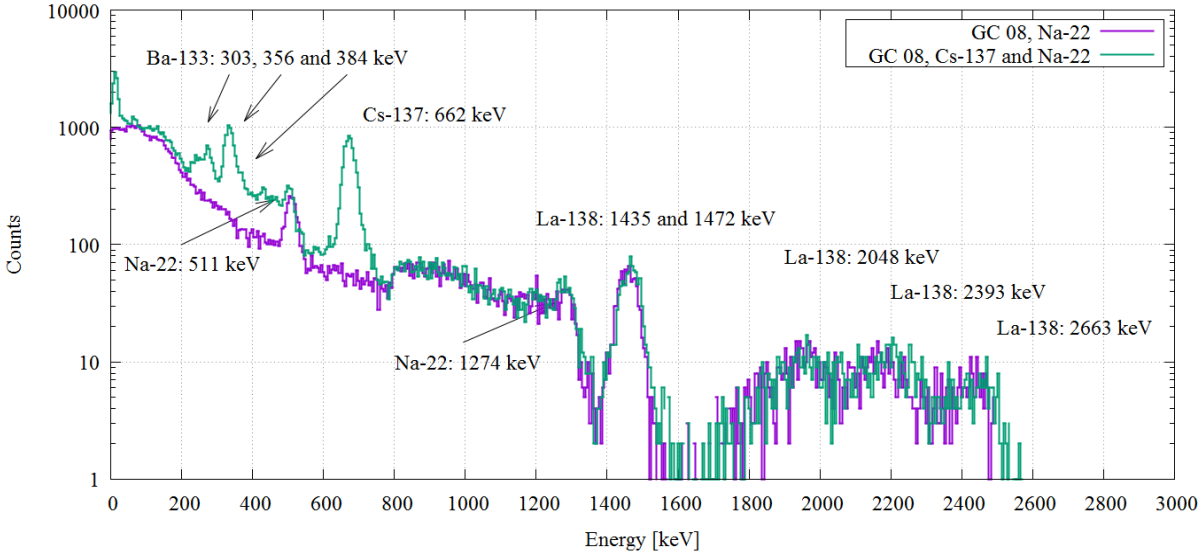

Fig 10. Gamma energy spectra of the GC 08.

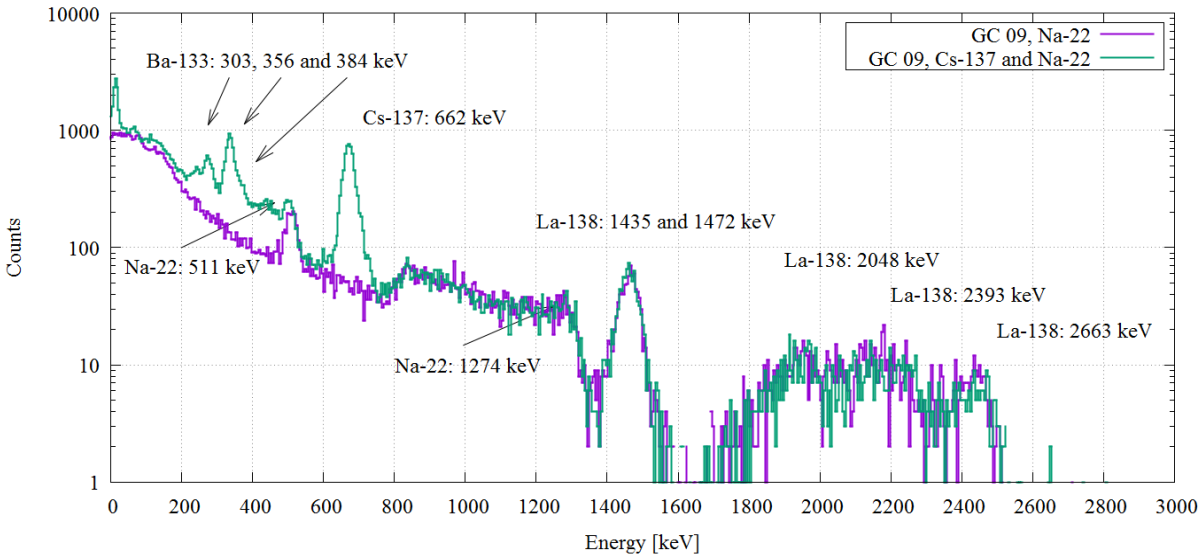

Fig 11. Gamma energy spectra of the GC 09.

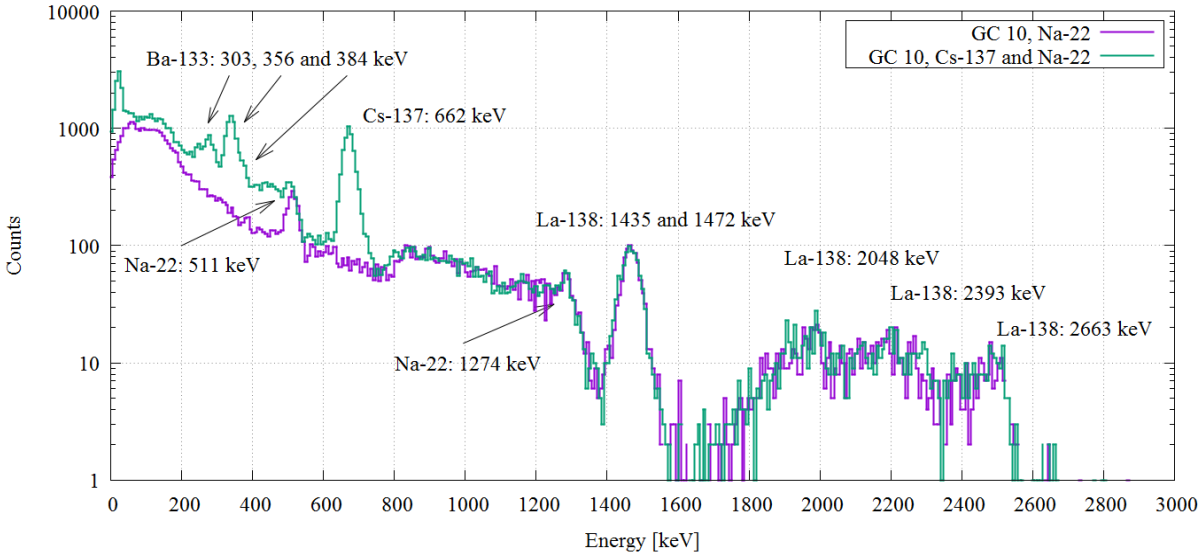

Fig 12. Gamma energy spectra of the GC 10.

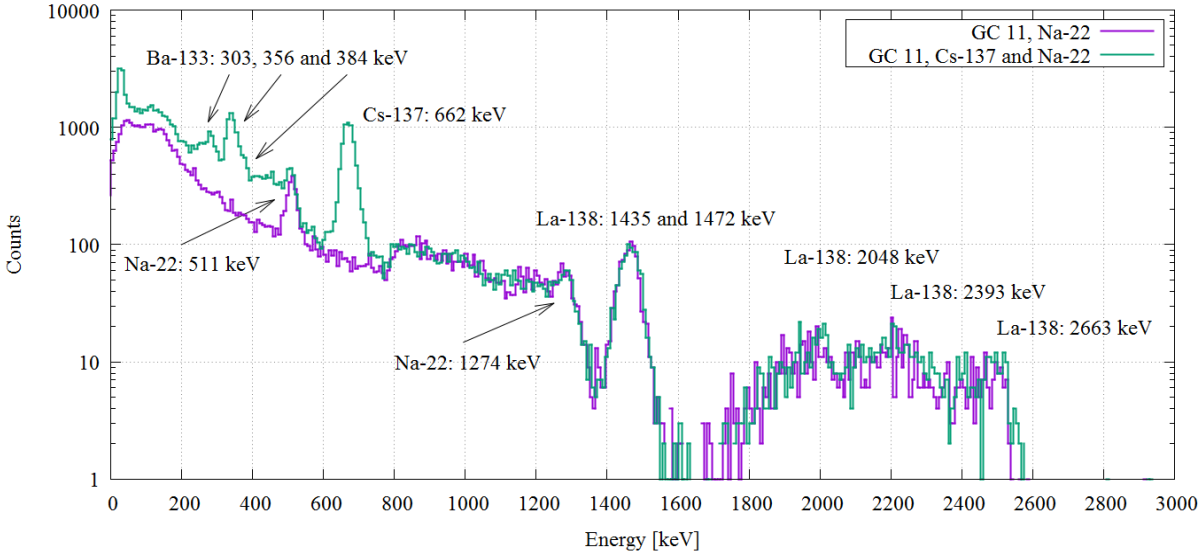

Fig 13. Gamma energy spectra of the GC 11.

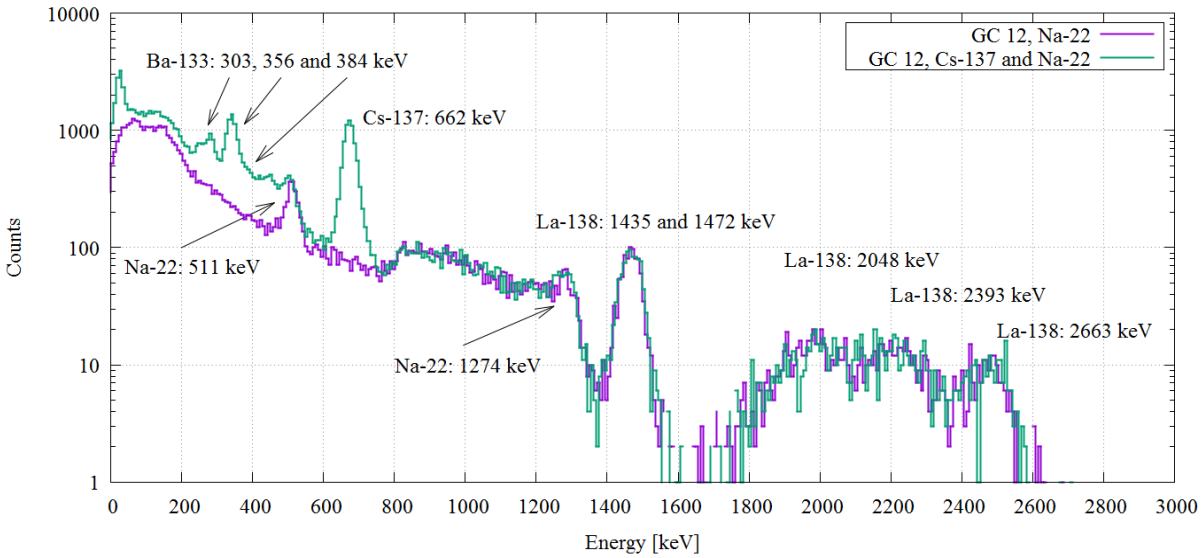

Fig 15. Gamma energy spectra of the GC 12.

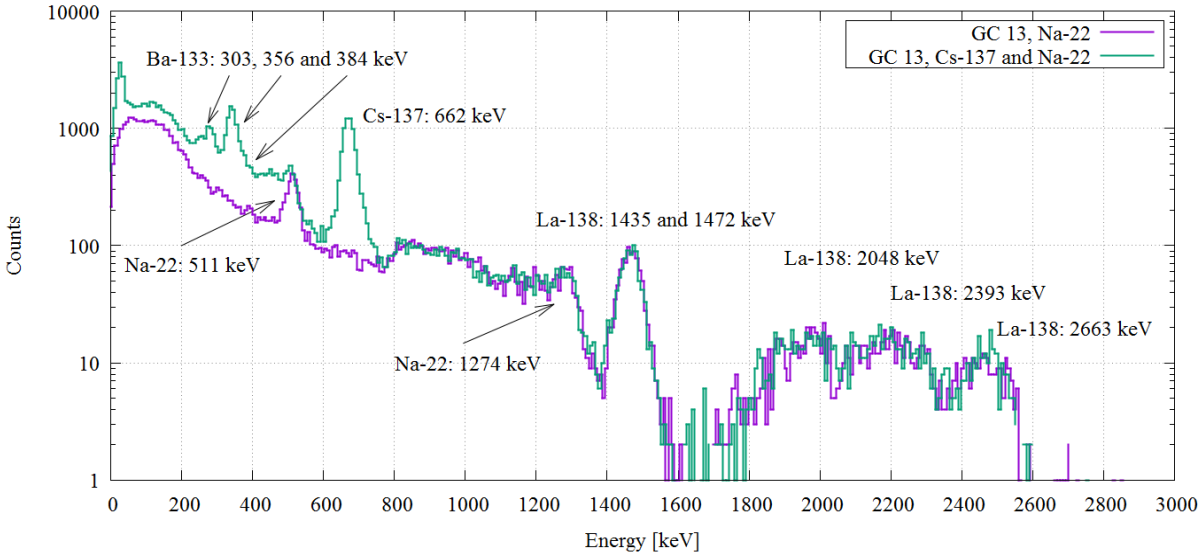

Fig 15. Gamma energy spectra of the GC 13.

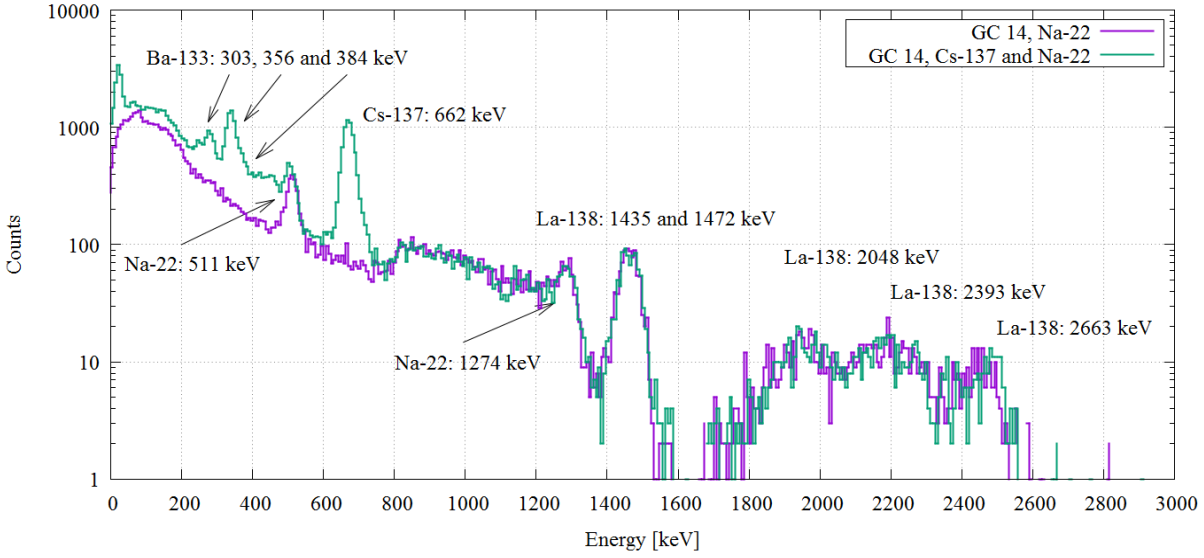

Fig 16. Gamma energy spectra of the GC 14.

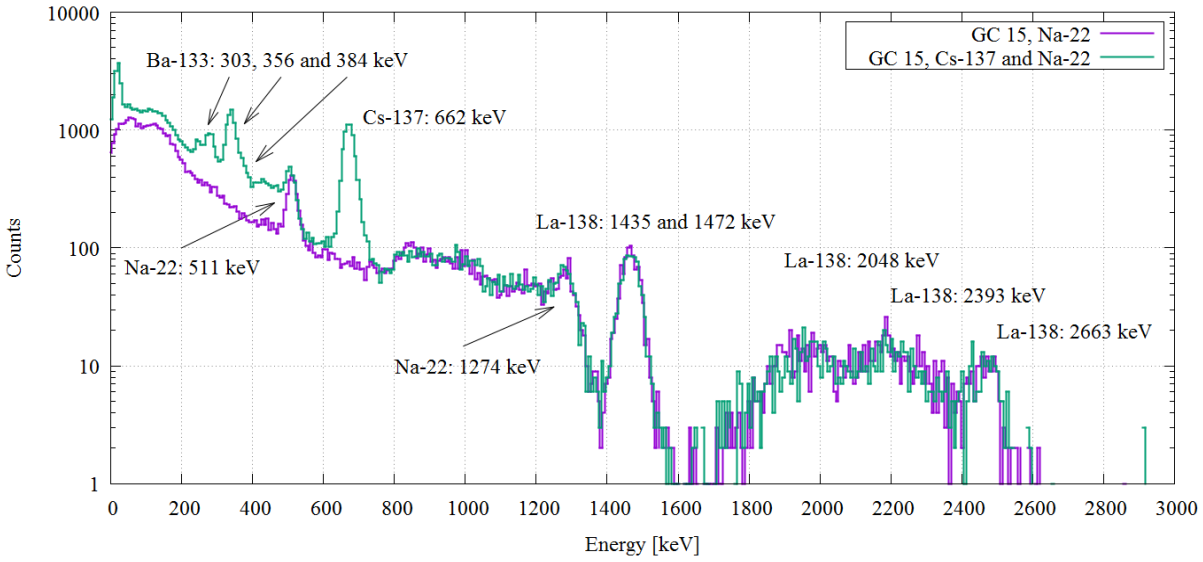

Fig 17. Gamma energy spectra of the GC 15.

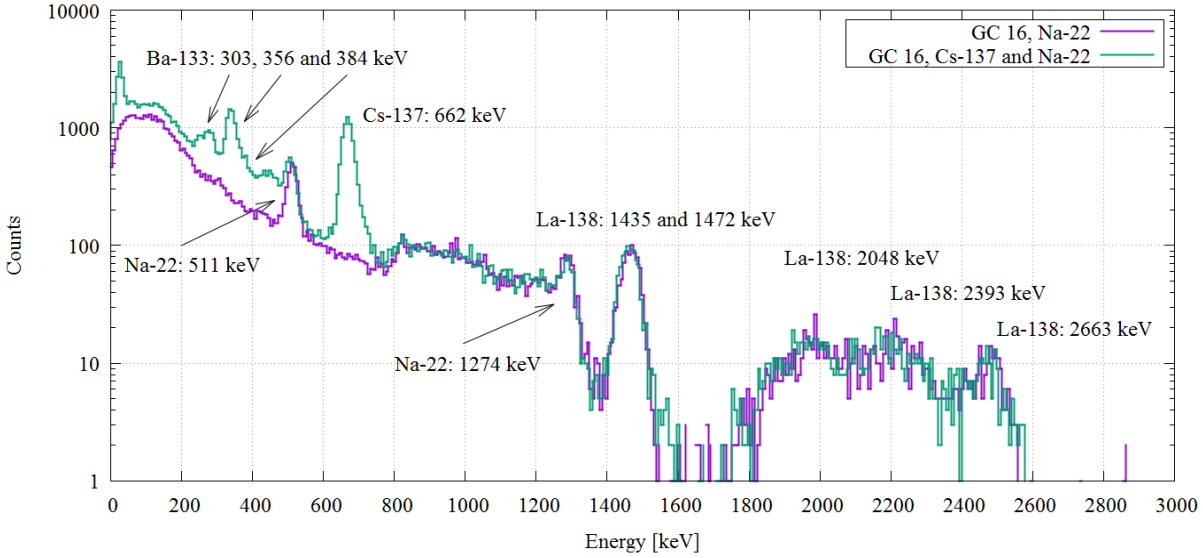

Fig 18. Gamma energy spectra of the GC 16.

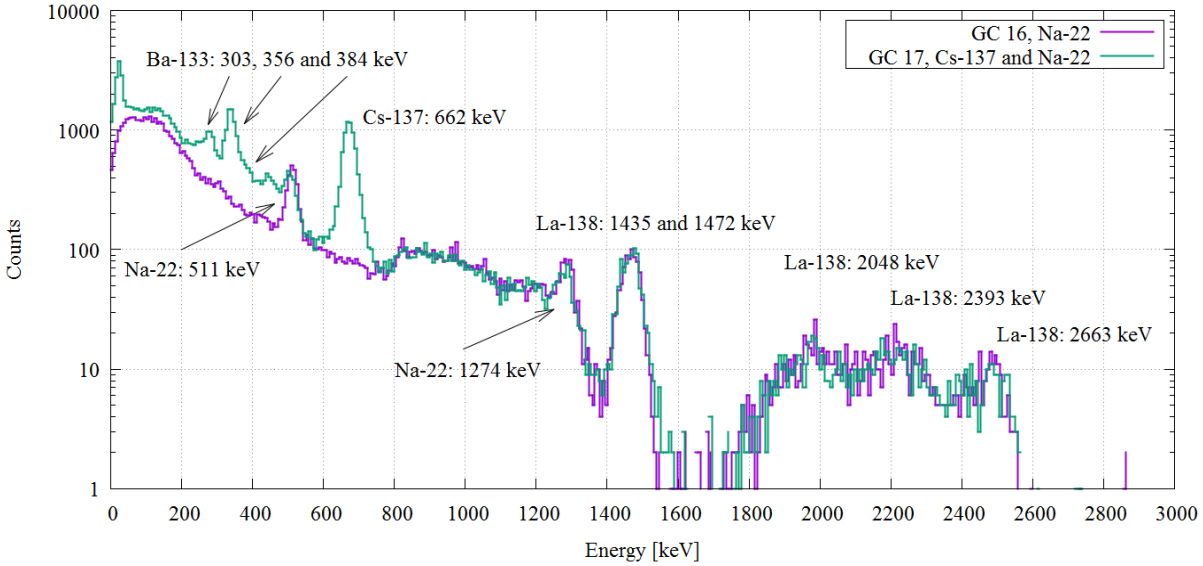

Fig 19. Gamma energy spectra of the GC 17.

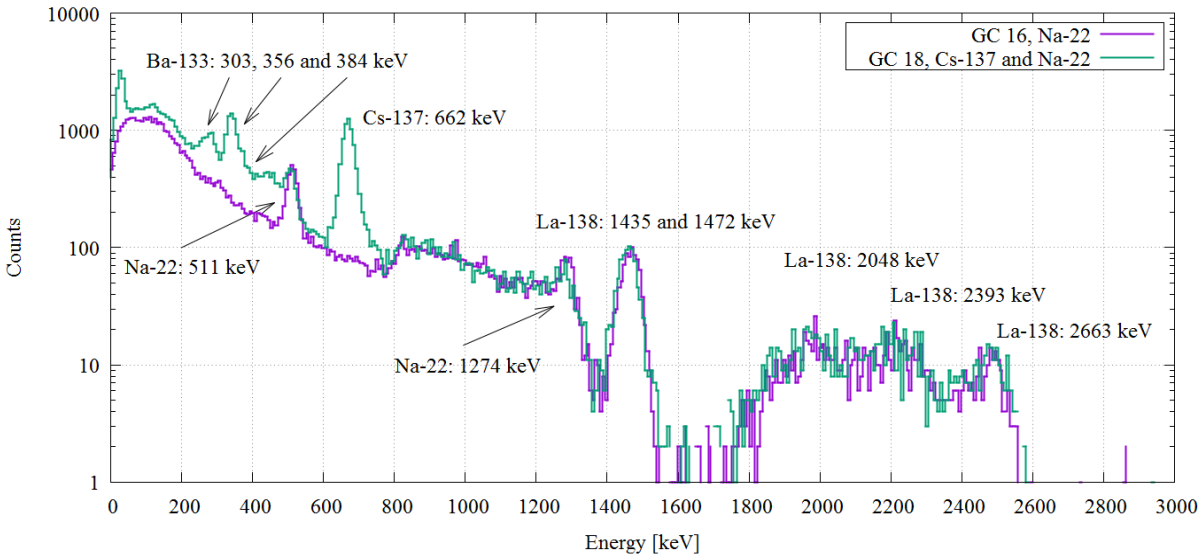

Fig 20. Gamma energy spectra of the GC 18.

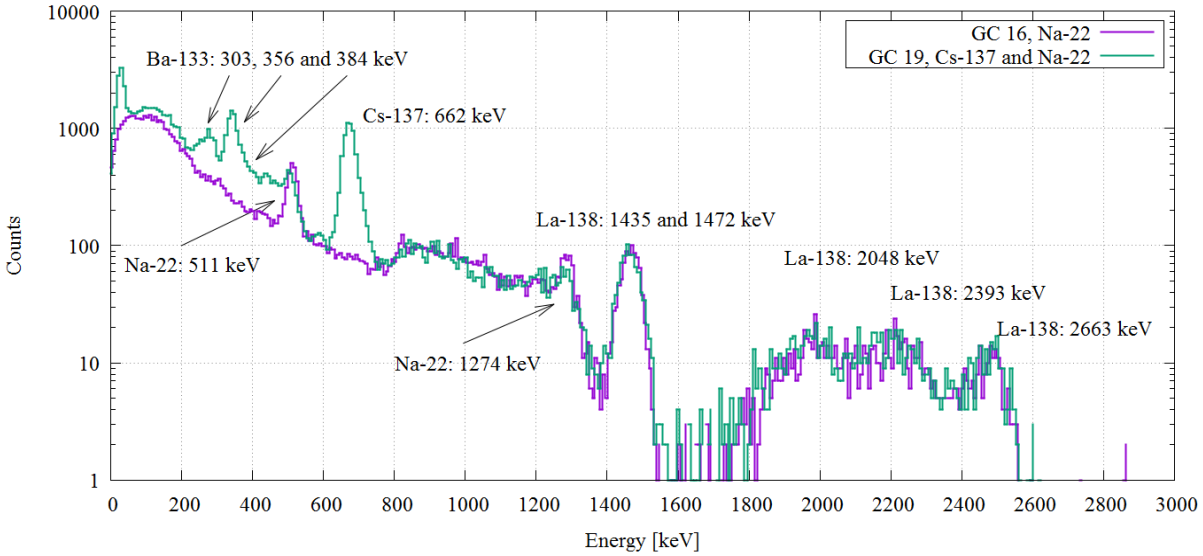

Fig 21. Gamma energy spectra of the GC 19.

6. Energy resolution at 662 keV

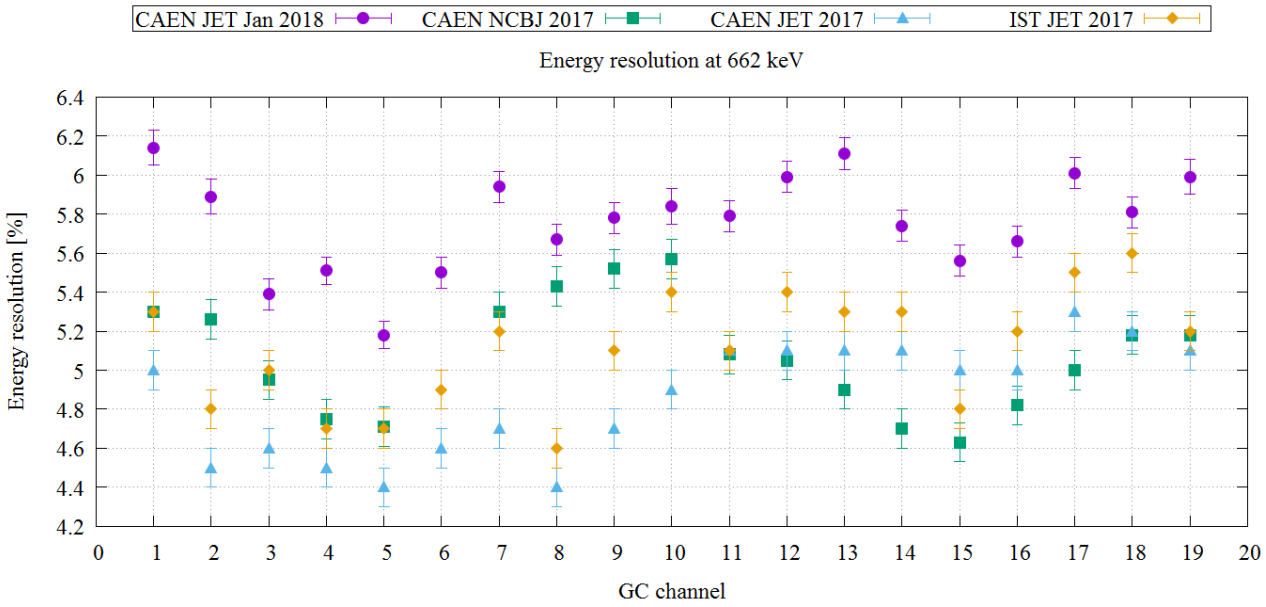

Fig. 22. Energy resolution at 662 keV for detectors installed in the Gamma Camera at JET (V=54.6 V).

The difference between results, obtained in 2017 and 2018, may be caused by long cables (≈100 m) used at JET facility and an additional noise source.

7. Measurements with the IST acquisition

Optimal voltage for each detector in Gamma Camera was determined.

Measurement specification:

data acquisition system: IST digitizer,
acquisition time: 3600s,
sources ^{133}Ba, ^{137}Cs and ^{22}Na.
Range of the MPPC voltage: from 54.0 V at 20°C to 56.0 V at 20°C with a step 0.2 V.

Each spectrum was calibrated with a straight line based on 4 peaks: 511 keV, 662 keV, 1274 keV and 1470 keV.

Energy resolution at 662 keV was computed and then a parabolic curve was fitted to data, see Figs. 23-41. Energy spectra after calibration are shown in Figs. 42 – 60. Due to problems with channels #09 and #15 during tests (cables, threshold) it was not possible to fit the parabola successfully.

Some DAQ parameters (e.g. threshold) were changed between measurements. It was not considered during data analysis.

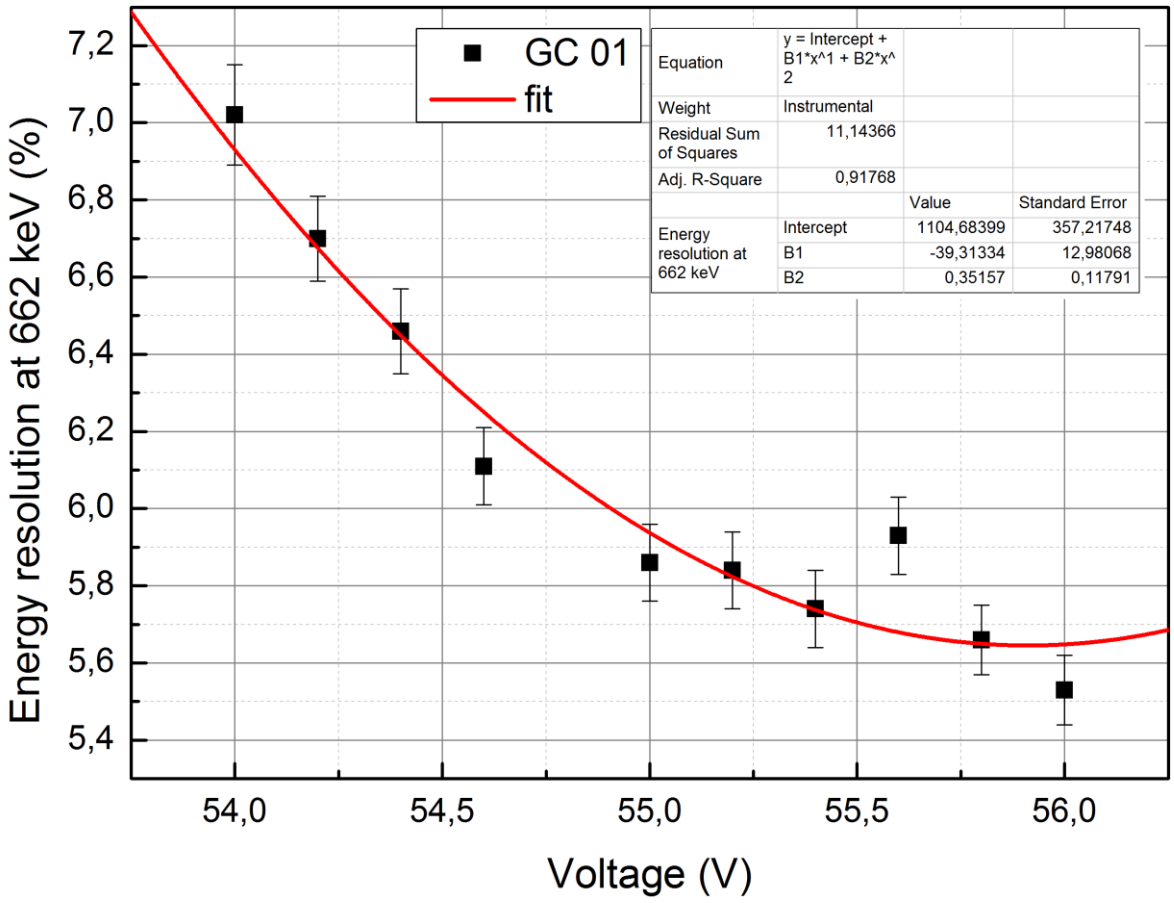

Fig. 23. Dependence energy resolution at 662 keV on MPPC voltage in GC channel 01.

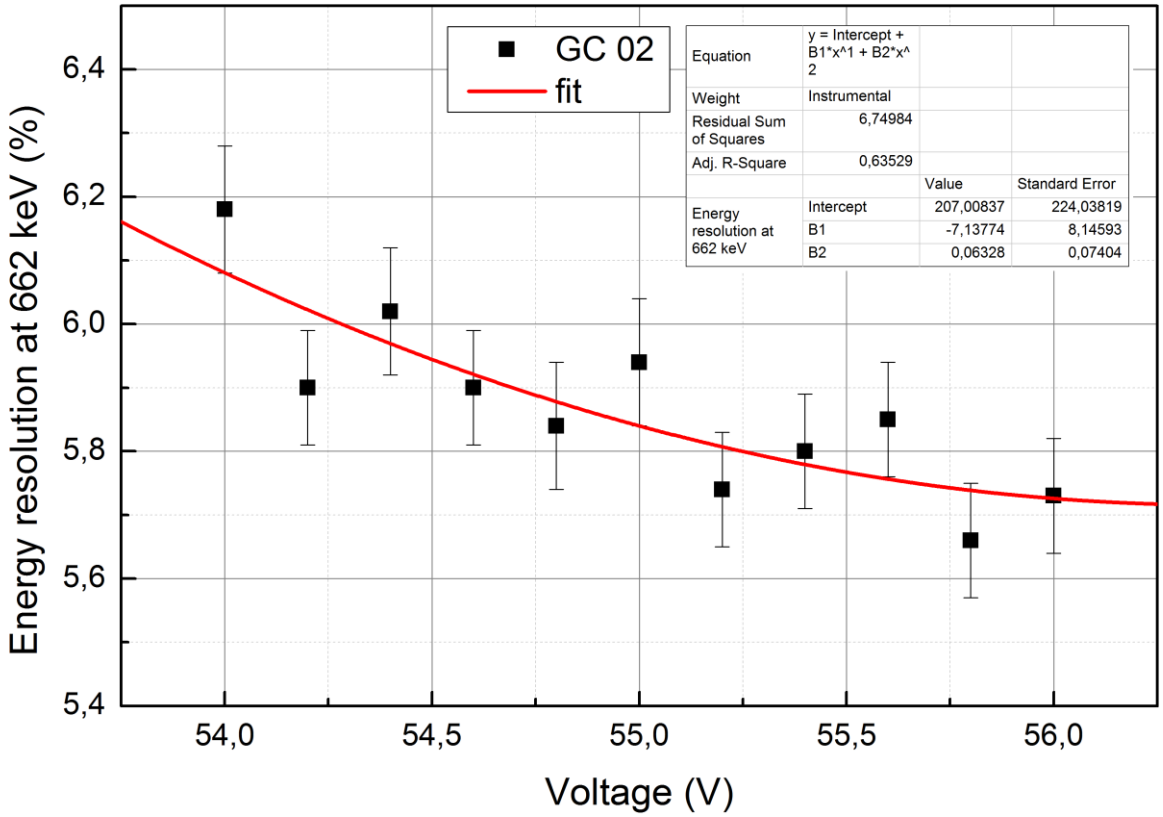

Fig. 24. Dependence energy resolution at 662 keV on MPPC voltage in GC channel 02.

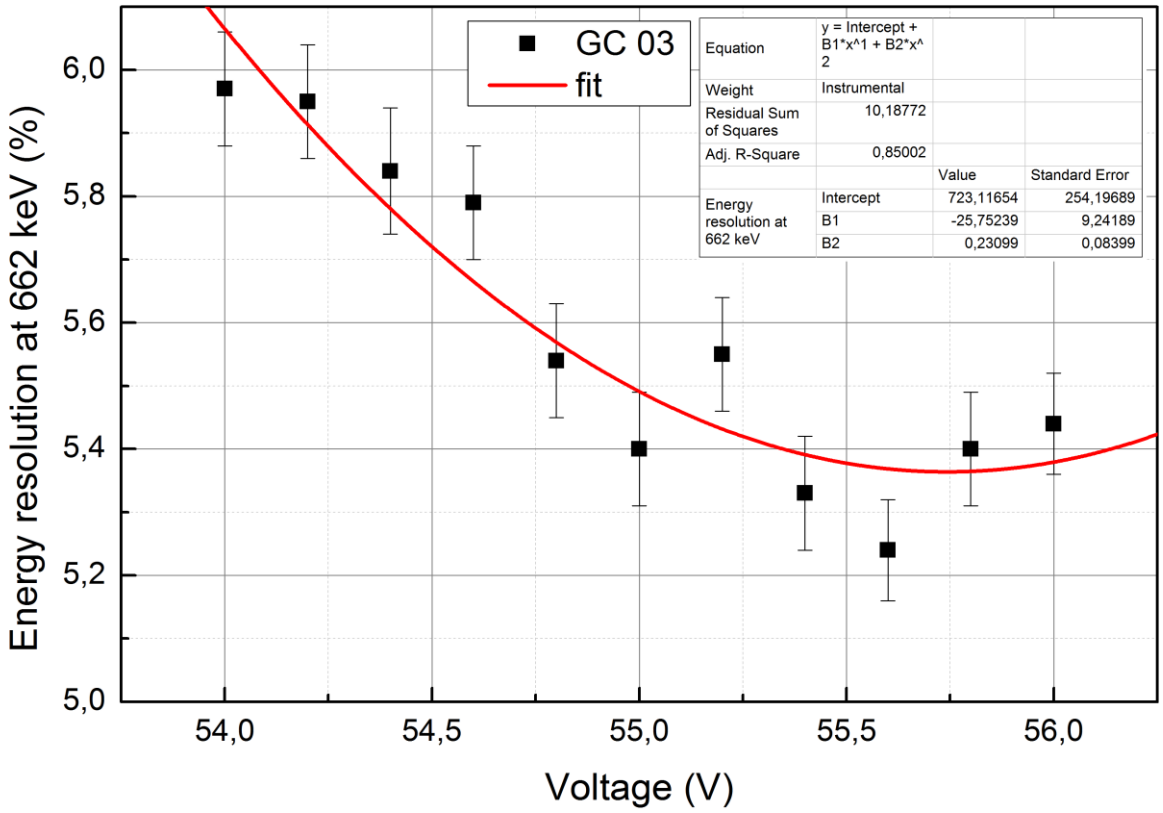

Fig. 25. Dependence energy resolution at 662 keV on MPPC voltage in GC channel 03.

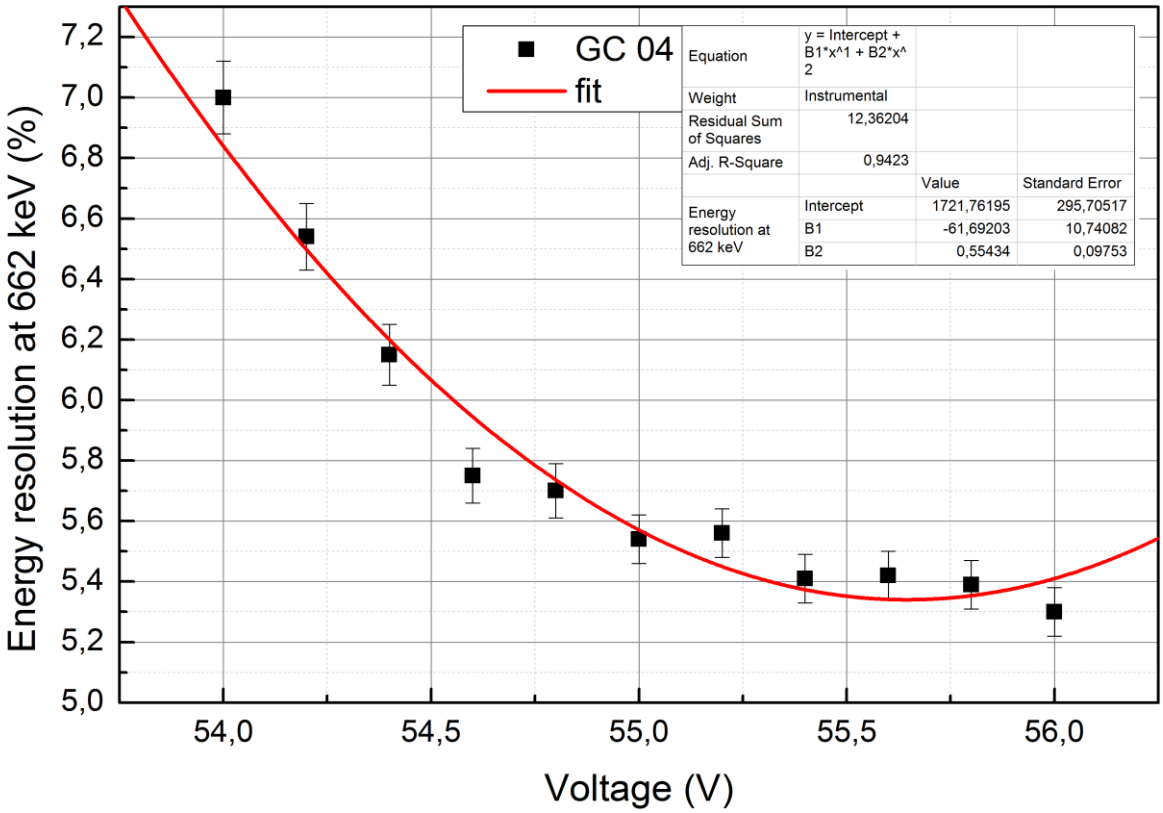

Fig. 26. Dependence energy resolution at 662 keV on MPPC voltage in GC channel 04.

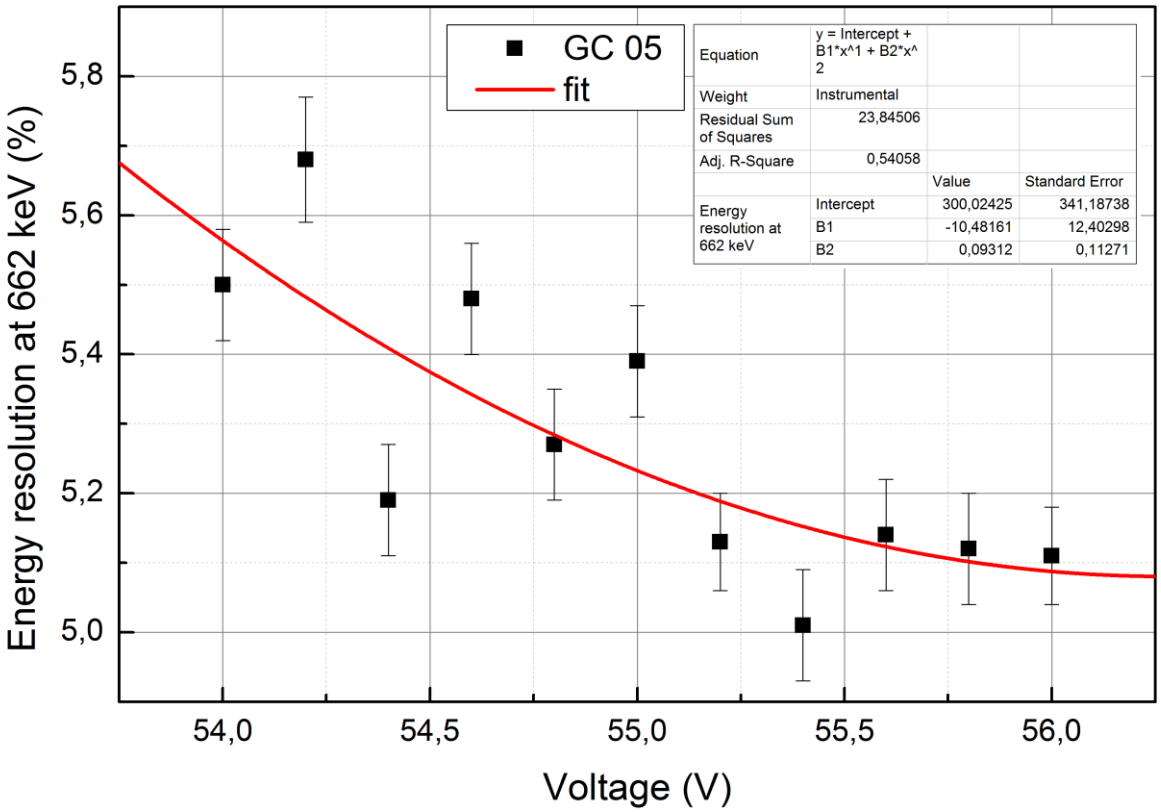

Fig. 27. Dependence energy resolution at 662 keV on MPPC voltage in GC channel 05.

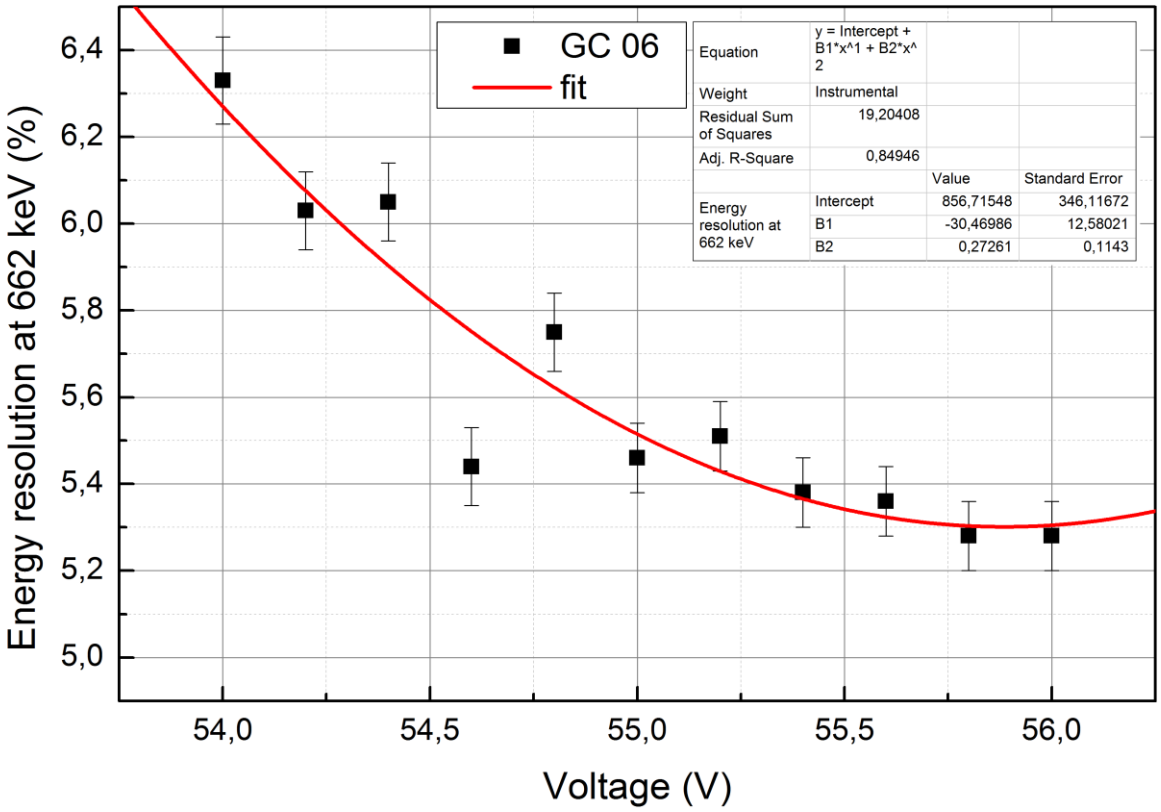

Fig. 28. Dependence energy resolution at 662 keV on MPPC voltage in GC channel 06.

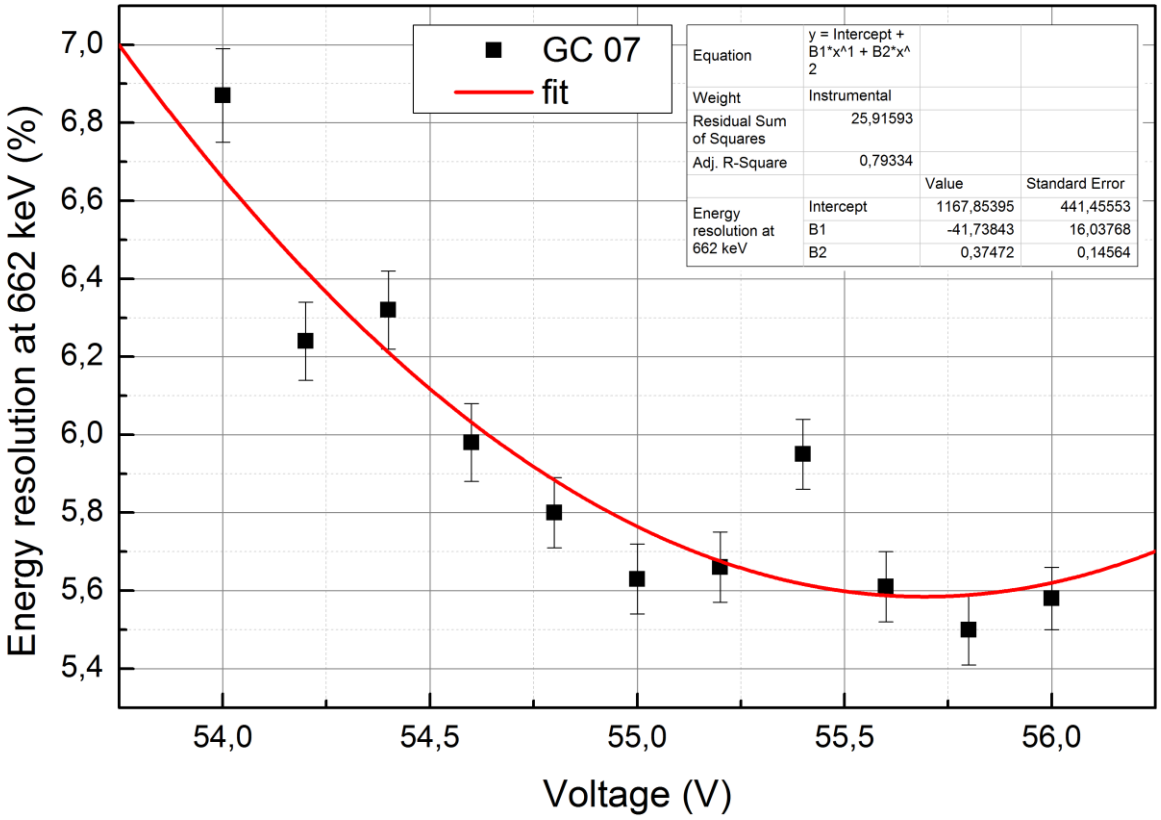

Fig. 29. Dependence energy resolution at 662 keV on MPPC voltage in GC channel 07.

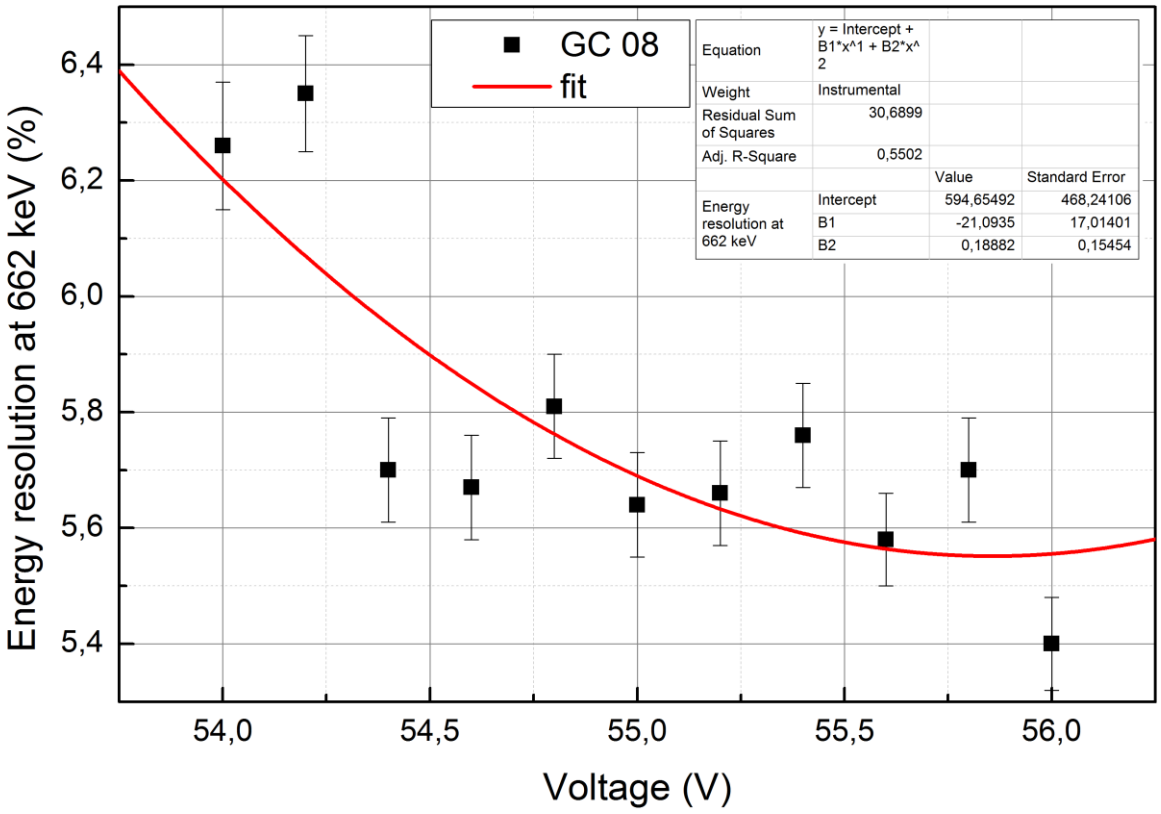

Fig. 30. Dependence energy resolution at 662 keV on MPPC voltage in GC channel 08.

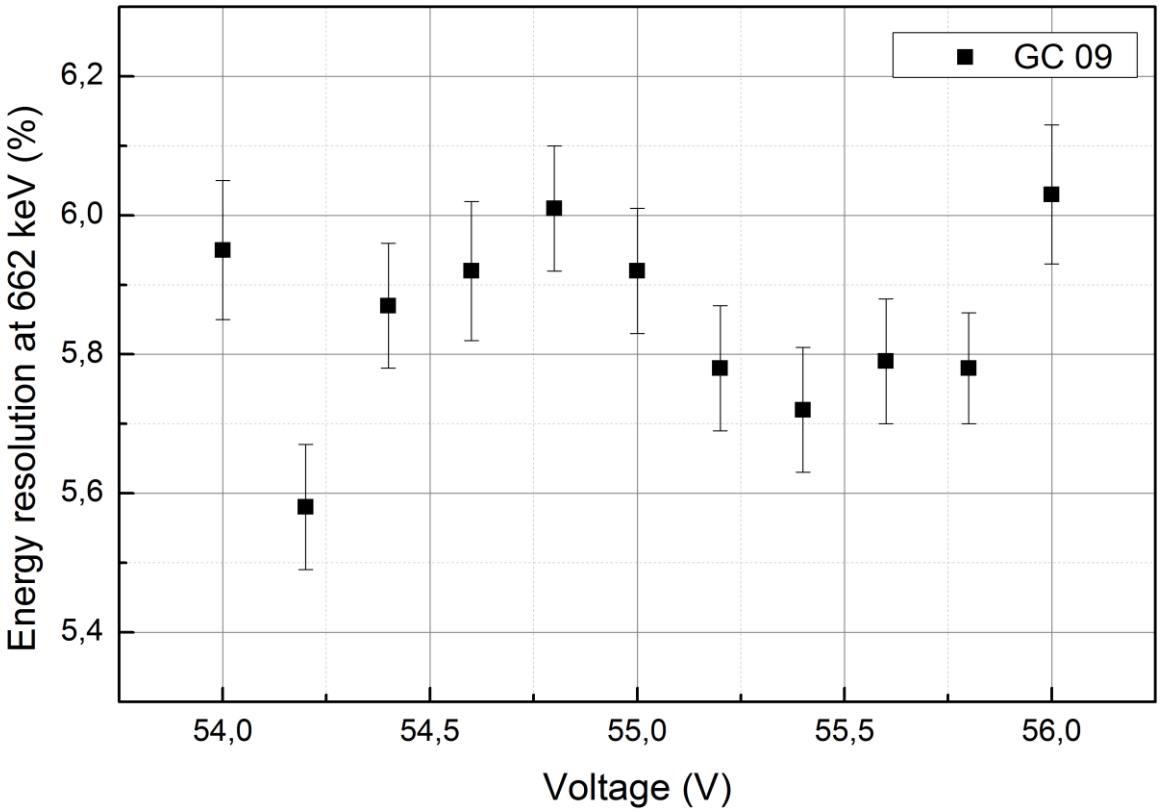

Fig. 31. Dependence energy resolution at 662 keV on MPPC voltage in GC channel 09.

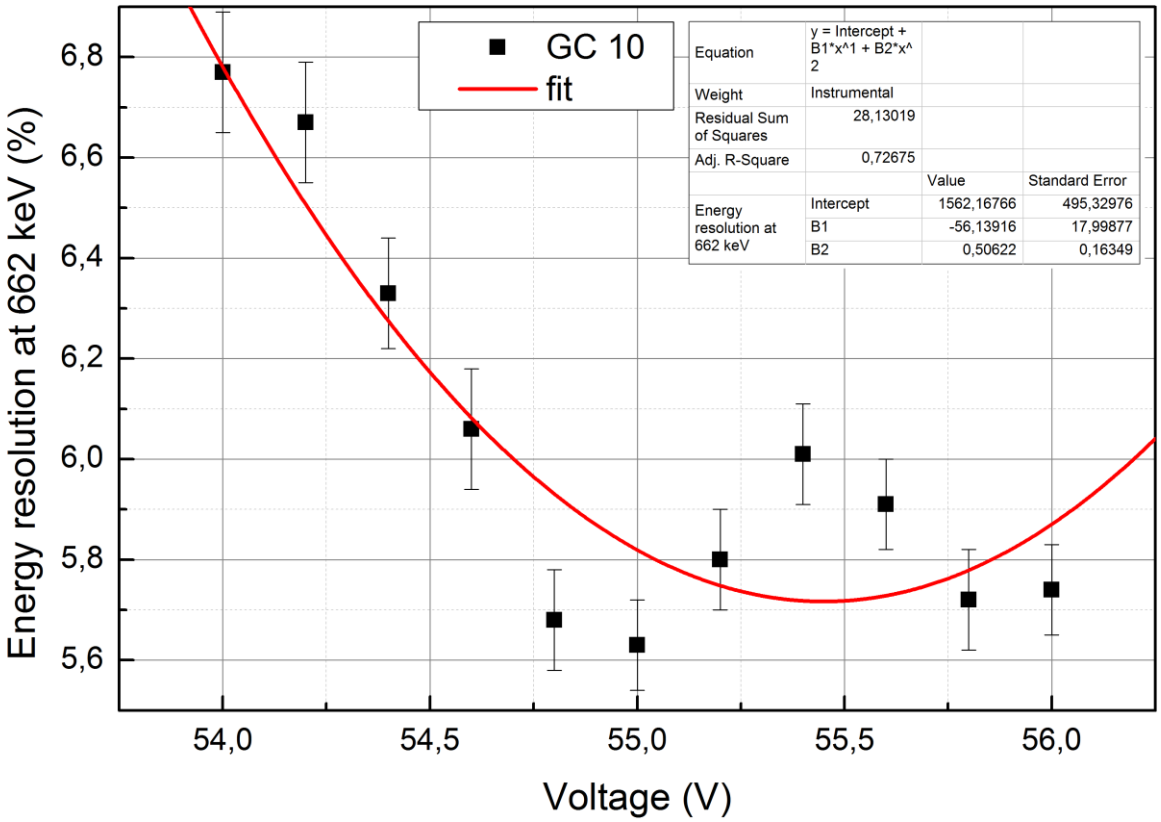

Fig. 32. Dependence energy resolution at 662 keV on MPPC voltage in GC channel 10.

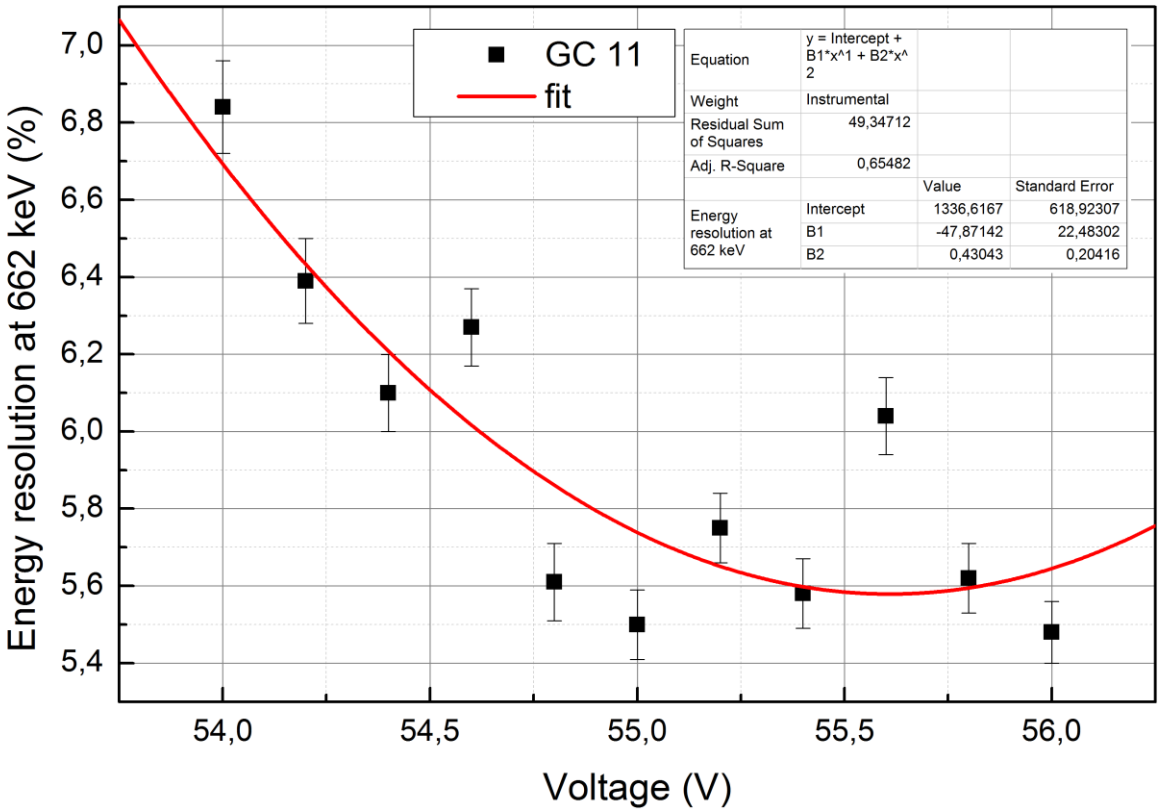

Fig. 33. Dependence energy resolution at 662 keV on MPPC voltage in GC channel 11.

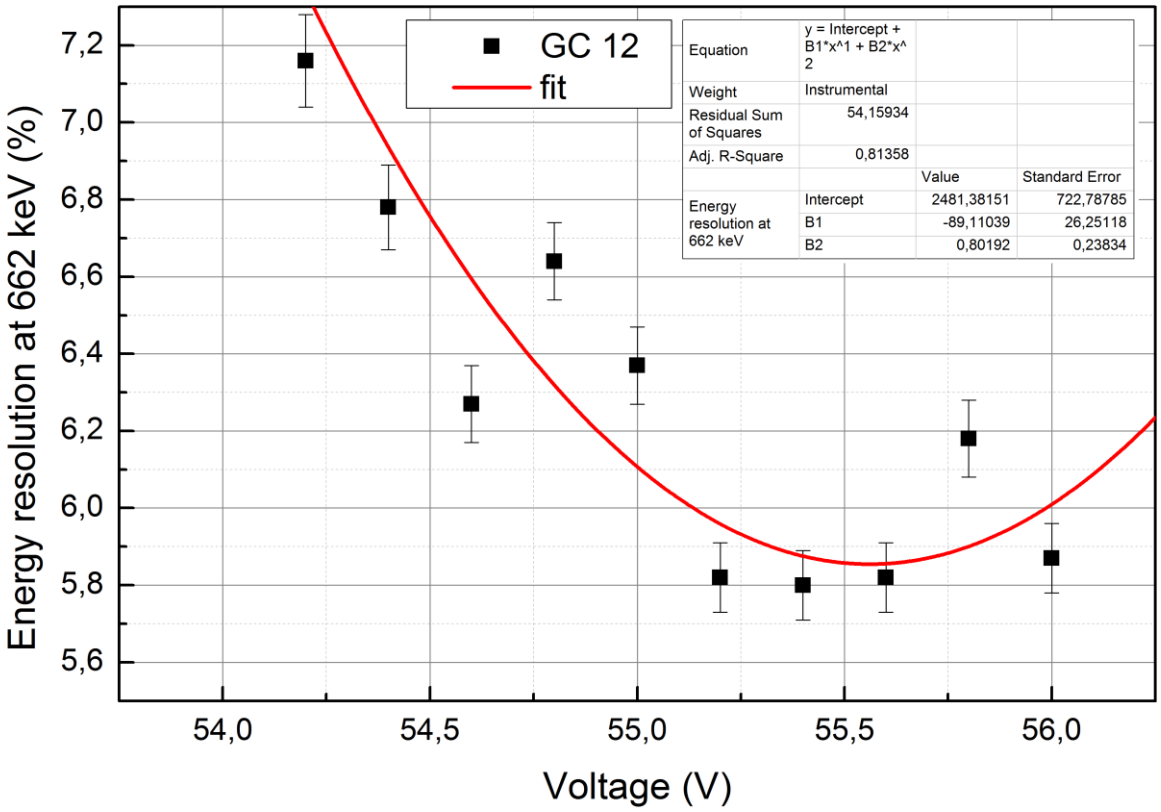

Fig. 34. Dependence energy resolution at 662 keV on MPPC voltage in GC channel 12.

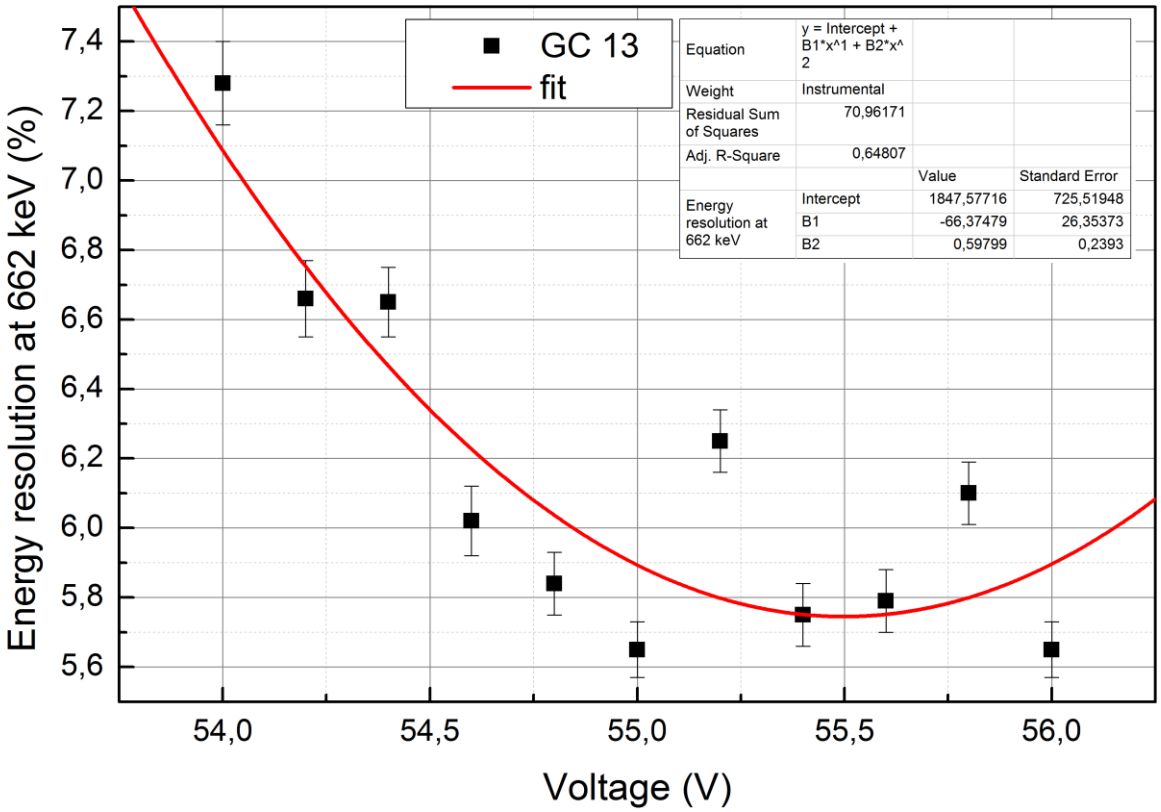

Fig. 35. Dependence energy resolution at 662 keV on MPPC voltage in GC channel 13.

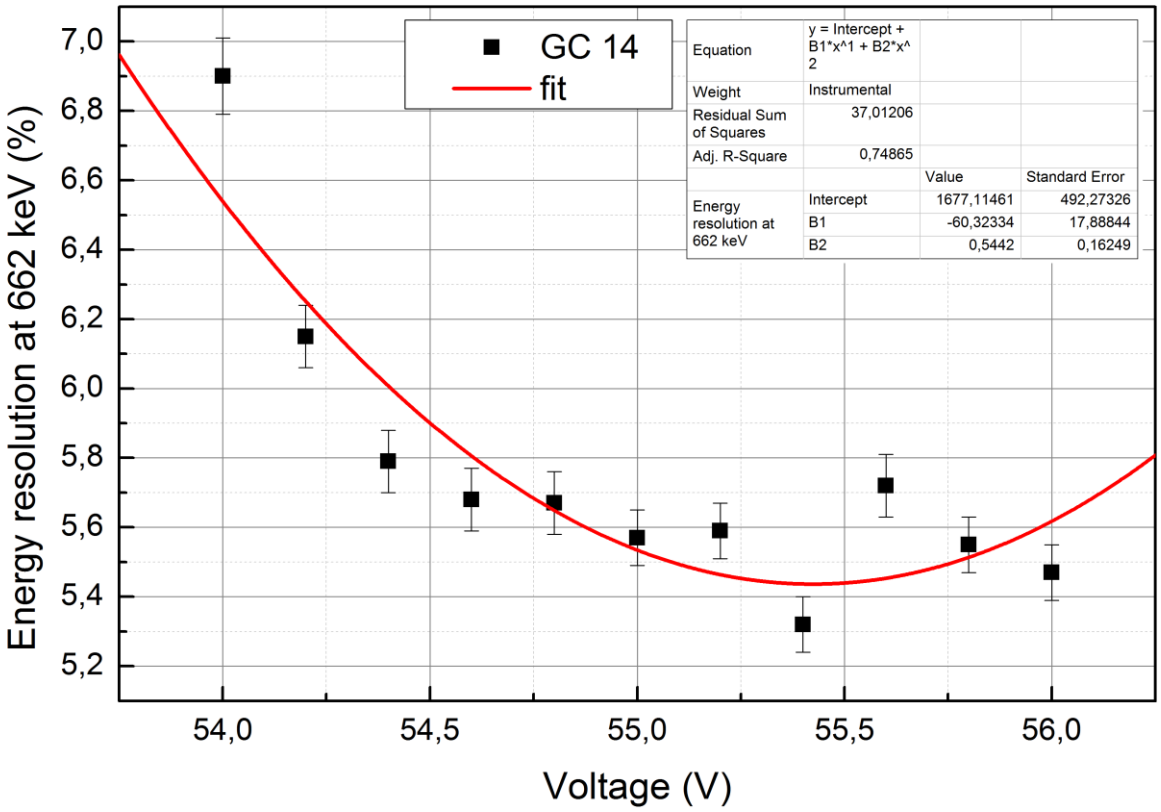

Fig. 36. Dependence energy resolution at 662 keV on MPPC voltage in GC channel 14.

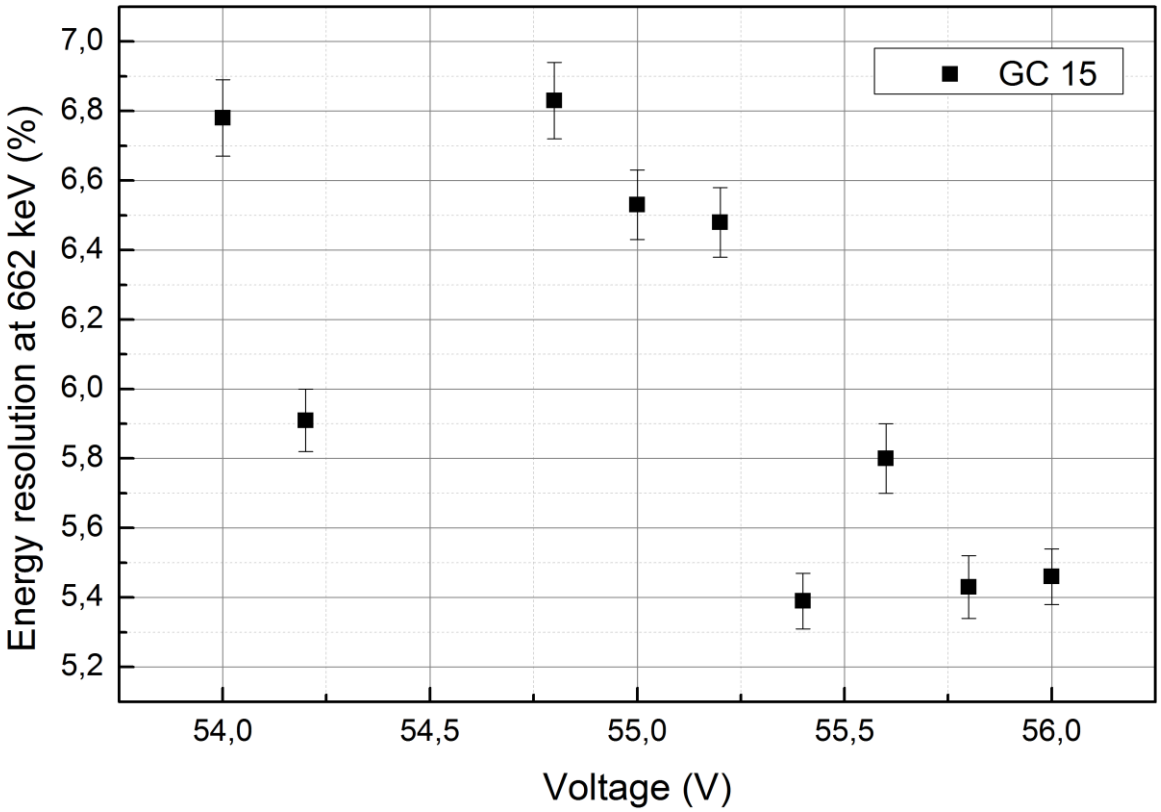

Fig. 37. Dependence energy resolution at 662 keV on MPPC voltage in GC channel 15.

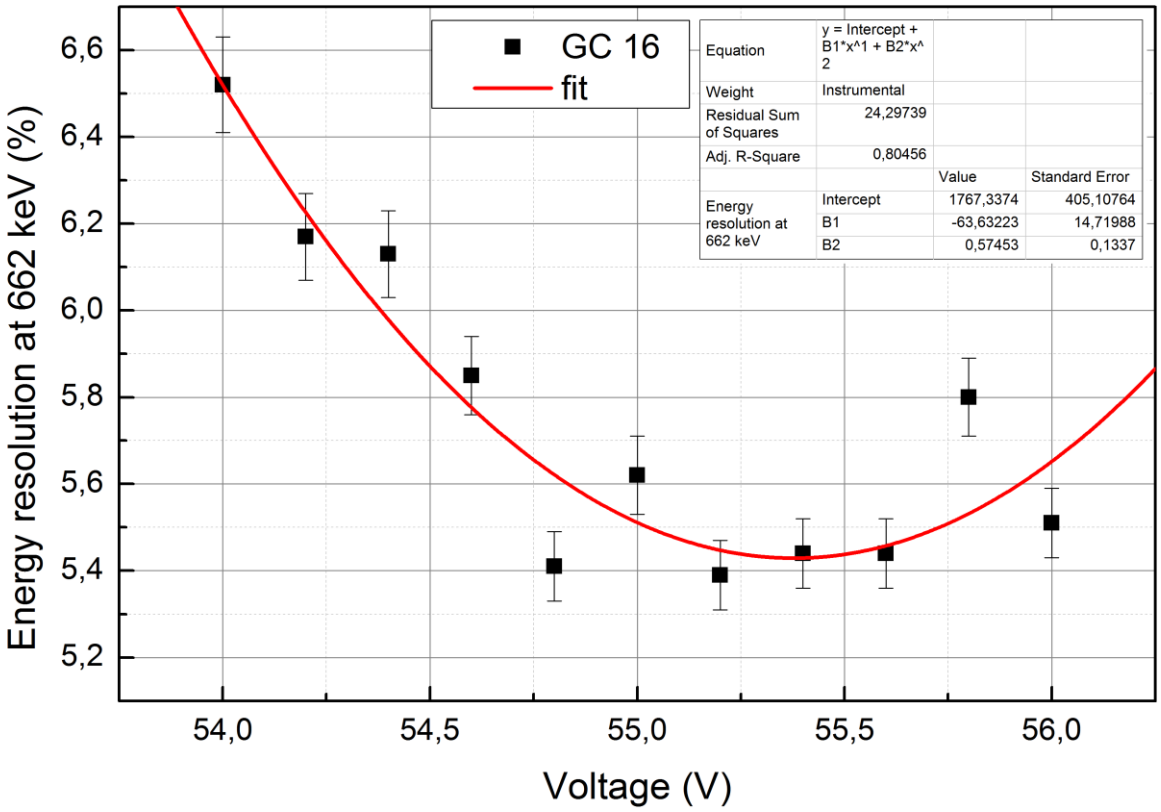

Fig. 38. Dependence energy resolution at 662 keV on MPPC voltage in GC channel 16.

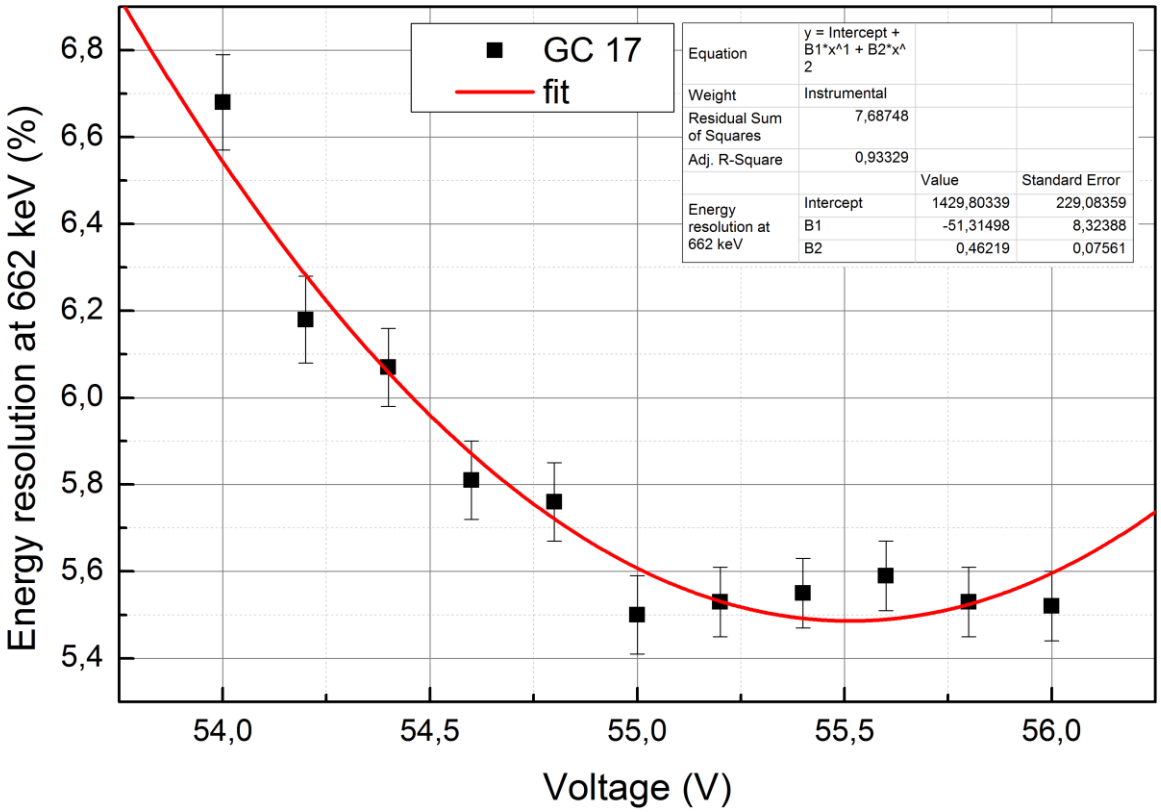

Fig. 39. Dependence energy resolution at 662 keV on MPPC voltage in GC channel 17.

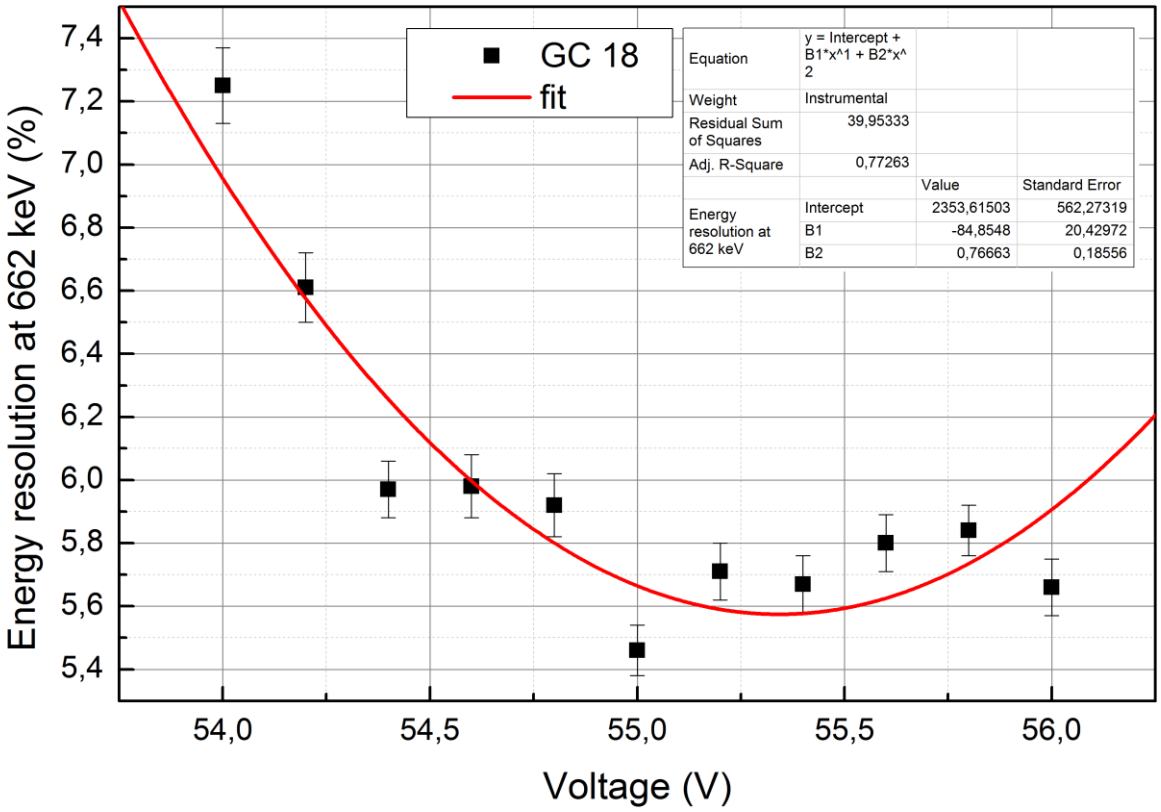

Fig. 40. Dependence energy resolution at 662 keV on MPPC voltage in GC channel 18.

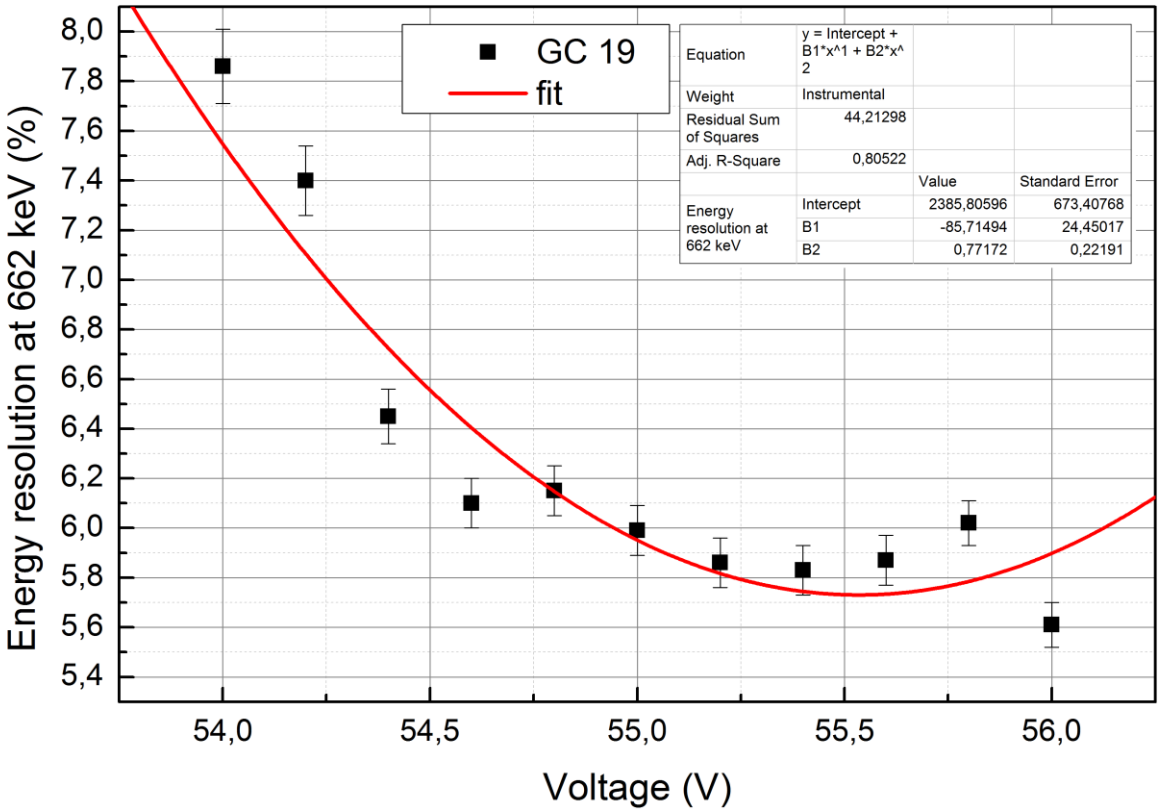

Fig. 41. Dependence energy resolution at 662 keV on MPPC voltage in GC channel 19.

8. Final tests

For each detector the optimal voltage was computed as the result of a parabola curve fit to the data presented in the previous paragraph. The optimal operational voltage is the abscissa of the parabola curve. The final measurement was performed with the IST DAQ with ^{133}Ba, ^{137}Cs and ^{22}Na sources, acquisition time was 3600 s. The linear calibration was done for each spectrum and all coefficients are presented in Table 4. The formula used for a calibration is $Energy\ [keV] = a_1 \times channel + a_0$

Table 4. Result of the measurement}

Channel No.	Voltage at 20 °C [V]	FWHM at 662 keV (fitted) [%]	FWHM at 662 keV (measured) [%]	Calibration coefficients	
				a_1	a_0
01	55.87	5.66	5.44 ± 0.09	4,151	7.022
02	56.40	5.72	5.78 ± 0.09	2.570	-66.48
03	55.74	5.37	5.41 ± 0.08	3.132	-0.20
04	55.65	5.34	5.27 ± 0.08	4.416	-67.58
05	56.28	5.08	5.11 ± 0.07	2.450	-71.87
06	55.89	5.30	5.29 ± 0.08	3.487	-40.07
07	55.69	5.58	5.91 ± 0.10	4.071	-24.65
08	55.86	5.55	5.39 ± 0.08	3.057	-36.61
09	55.40	5.85	5.95 ± 0.09	3.310	-68.14
10	55.45	5.72	6.04 ± 0.10	4.569	-64.46
11	55.61	5.58	5.38 ± 0.08	4.310	43.40
12	55.56	5.85	5.53 ± 0.08	4.350	-9.99
13	55.50	5.75	5.55 ± 0.09	4.740	16.14
14	55.42	5.44	5.79 ± 0.09	4.390	13.58
15	55.60	5.80	5.21 ± 0.08	4.060	-128.4
16	55.38	5.43	5.52 ± 0.08	4.630	73.19
17	55.51	5.48	5.74 ± 0.08	4.440	124.0
18	55.34	5.58	5.54 ± 0.08	4.950	71.03
19	55.54	5.75	6.00 ± 0.10	4.590	-48.45

In Figs. 42-60 all spectra obtained during the last measurement. are presented.

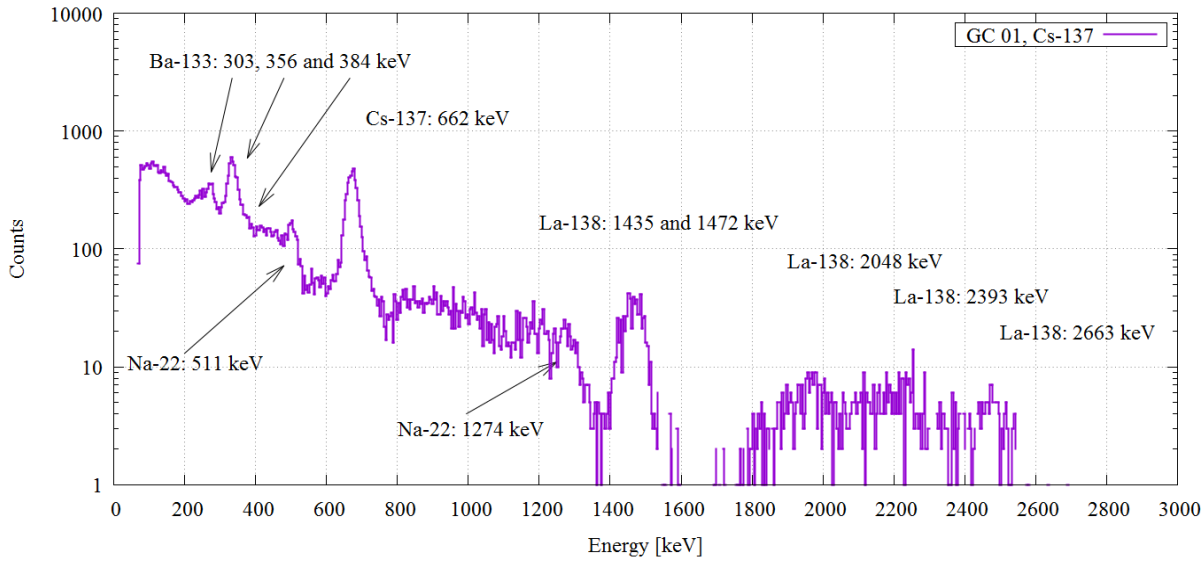

Fig. 42. Gamma spectrum in GC channel 01.

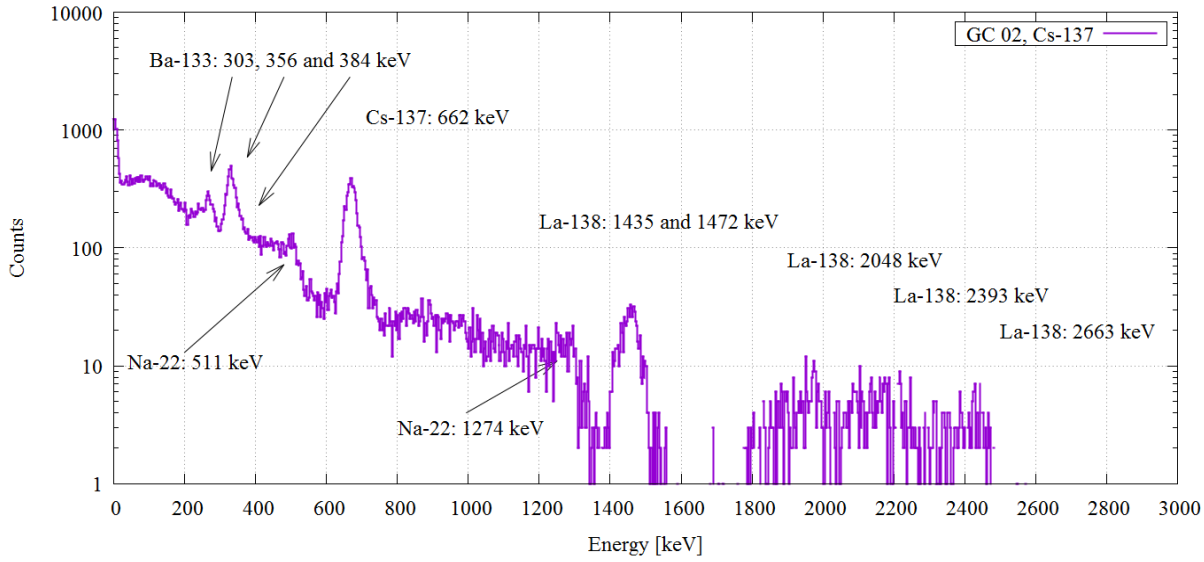

Fig. 43. Gamma spectrum in GC channel 02.

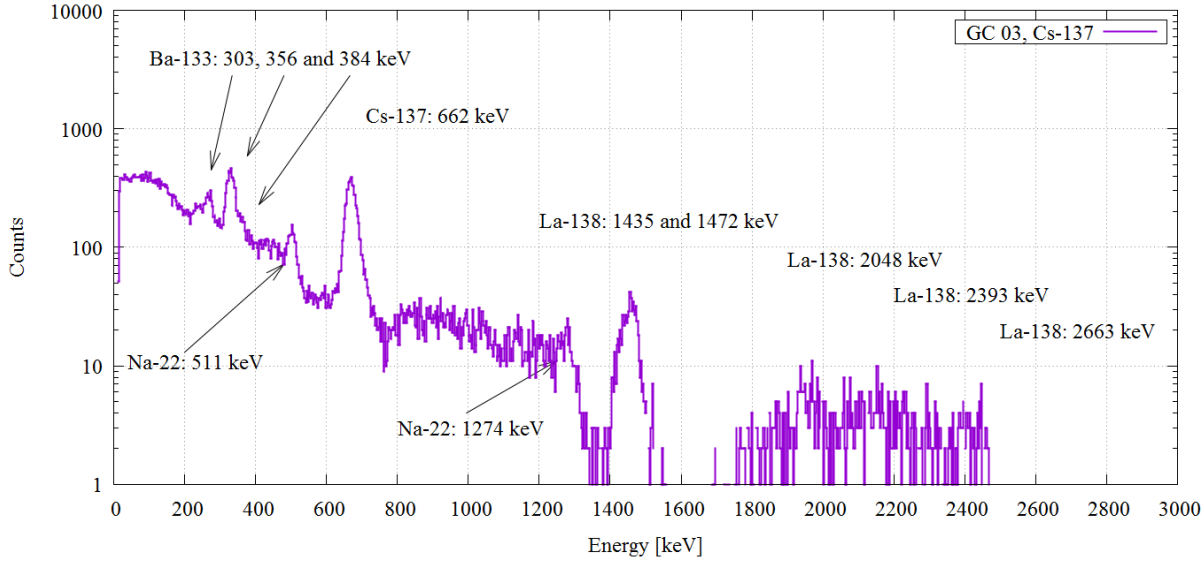

Fig. 44. Gamma spectrum in GC channel 03.

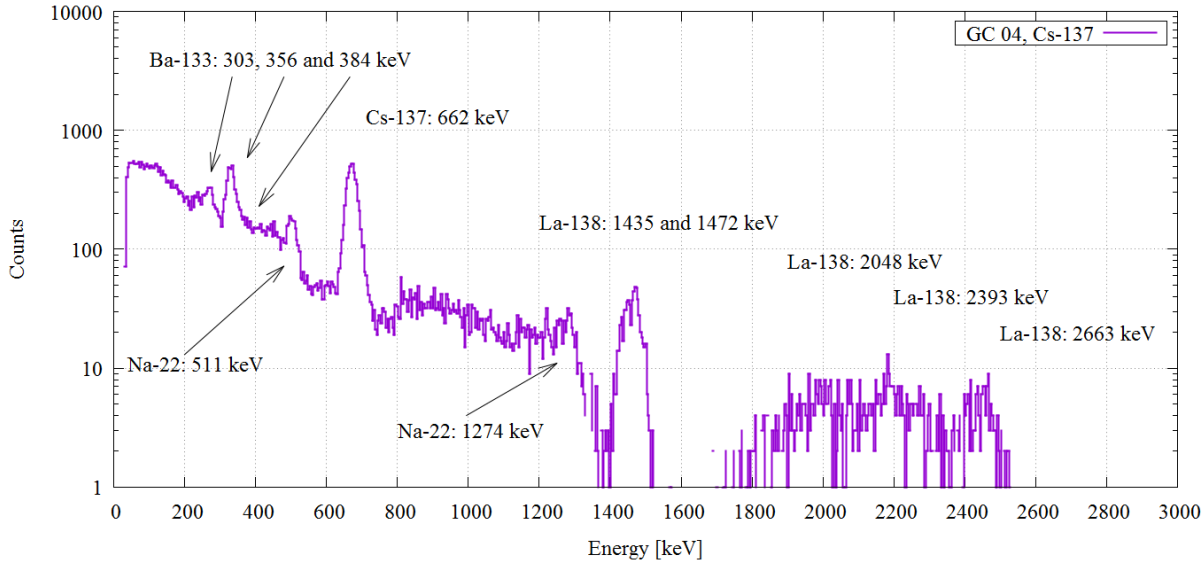

Fig. 45. Gamma spectrum in GC channel 04.

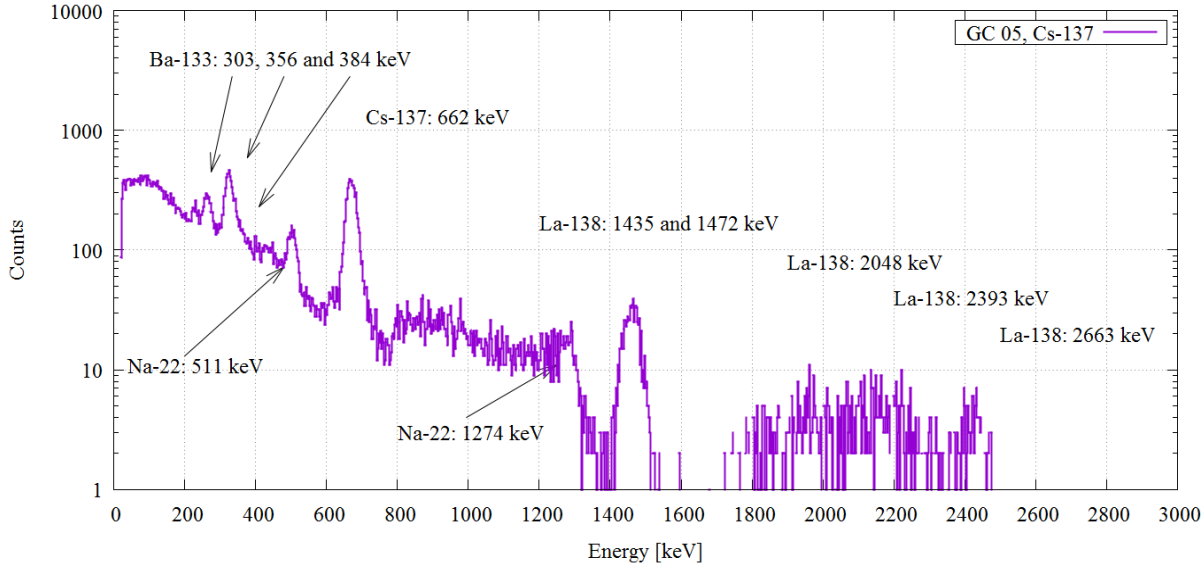

Fig. 46. Gamma spectrum in GC channel 05.

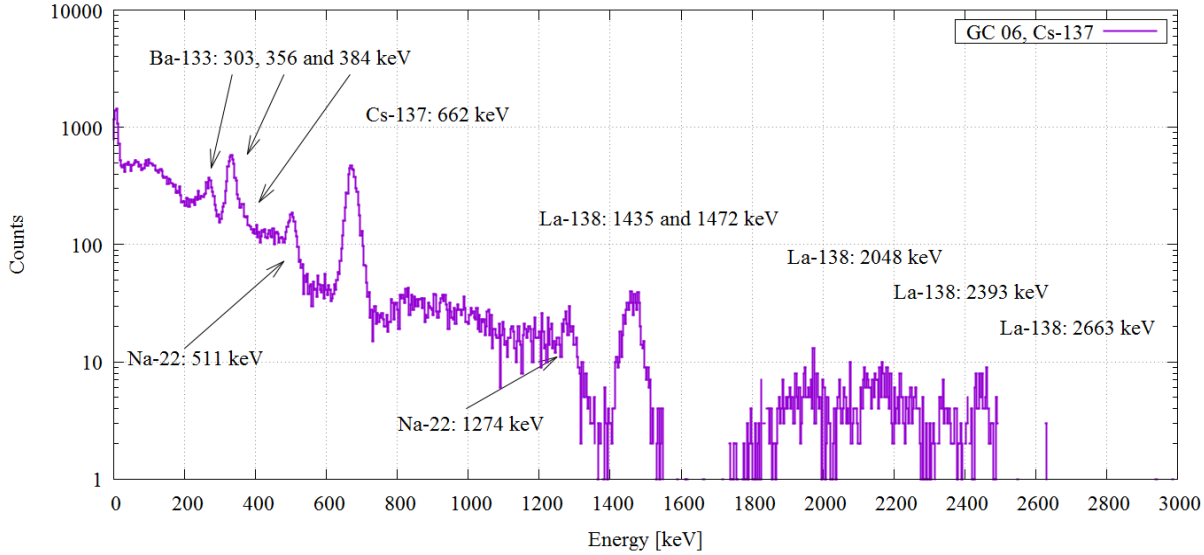

Fig. 47. Gamma spectrum in GC channel 06.

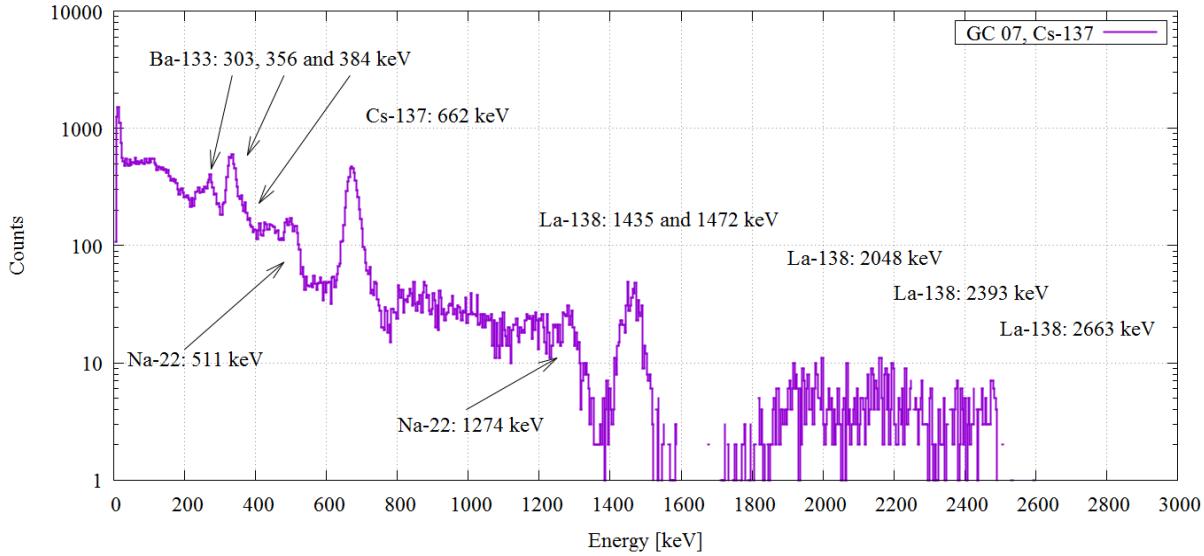

Fig. 48. Gamma spectrum in GC channel 07.

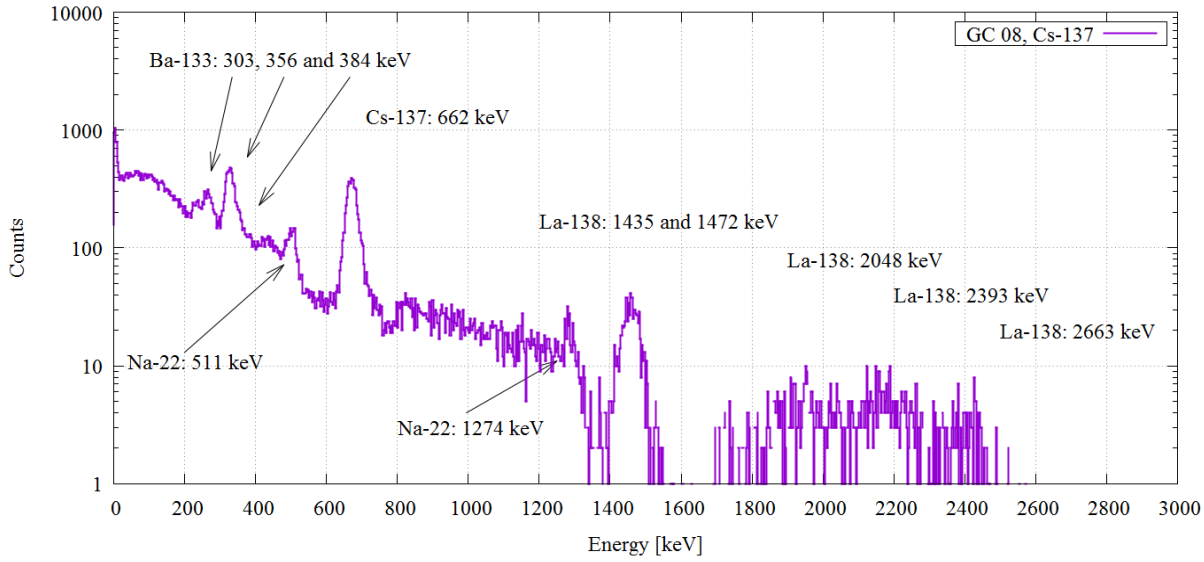

Fig. 49. Gamma spectrum in GC channel 08.

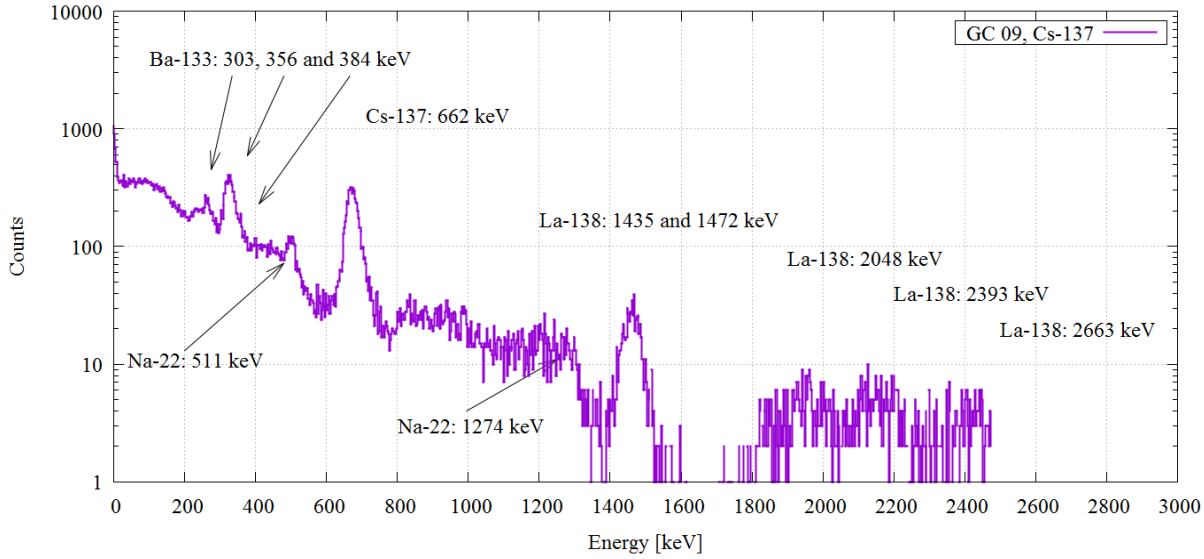

Fig. 50. Gamma spectrum in GC channel 09.

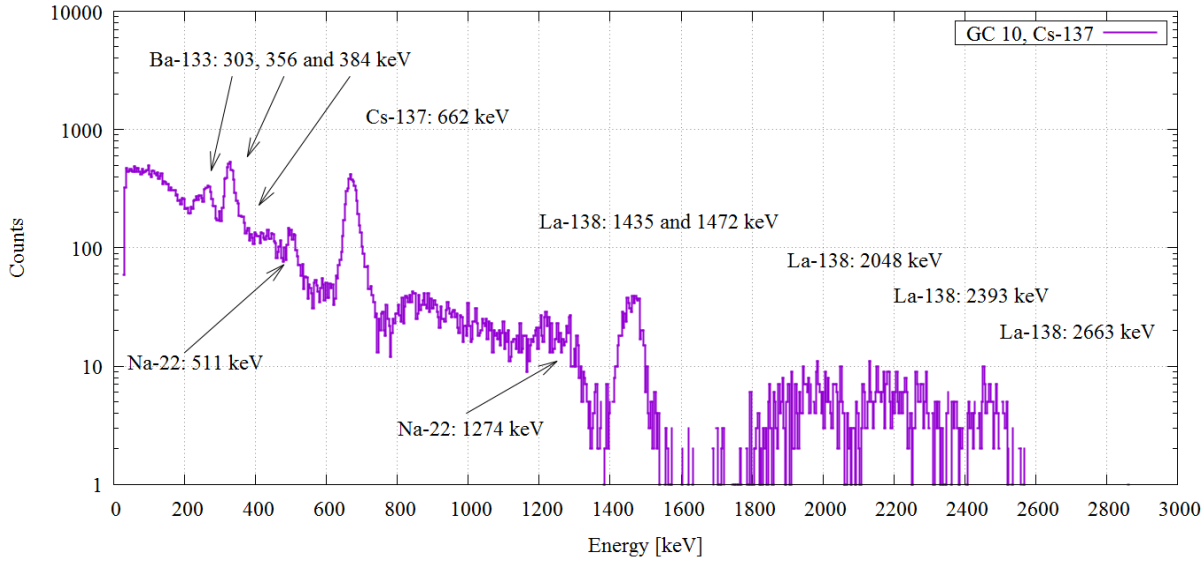

Fig. 51. Gamma spectrum in GC channel 10.

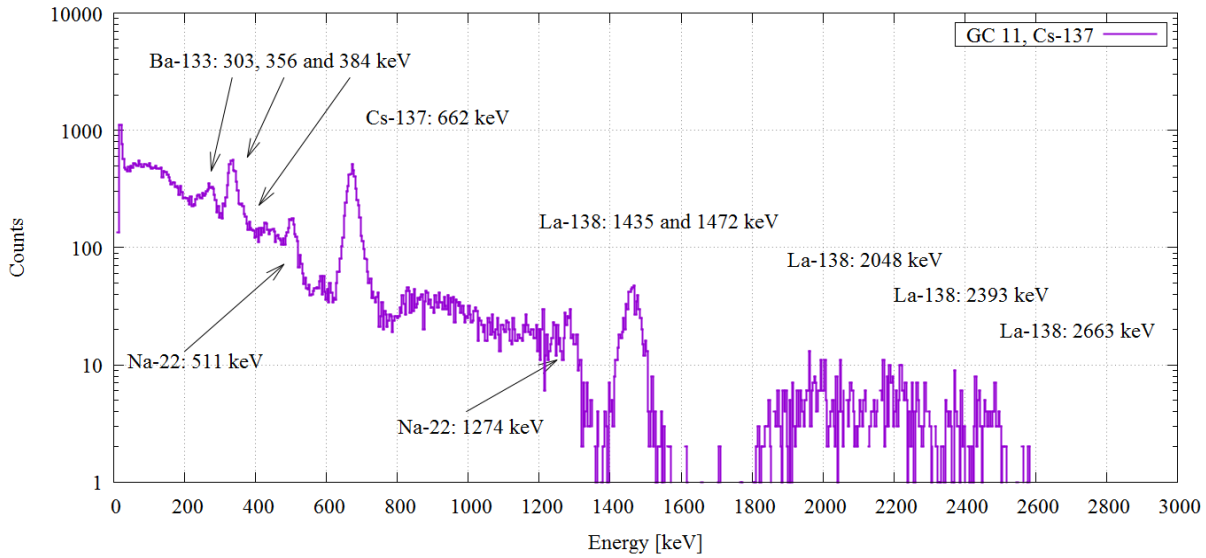

Fig. 52. Gamma spectrum in GC channel 11.

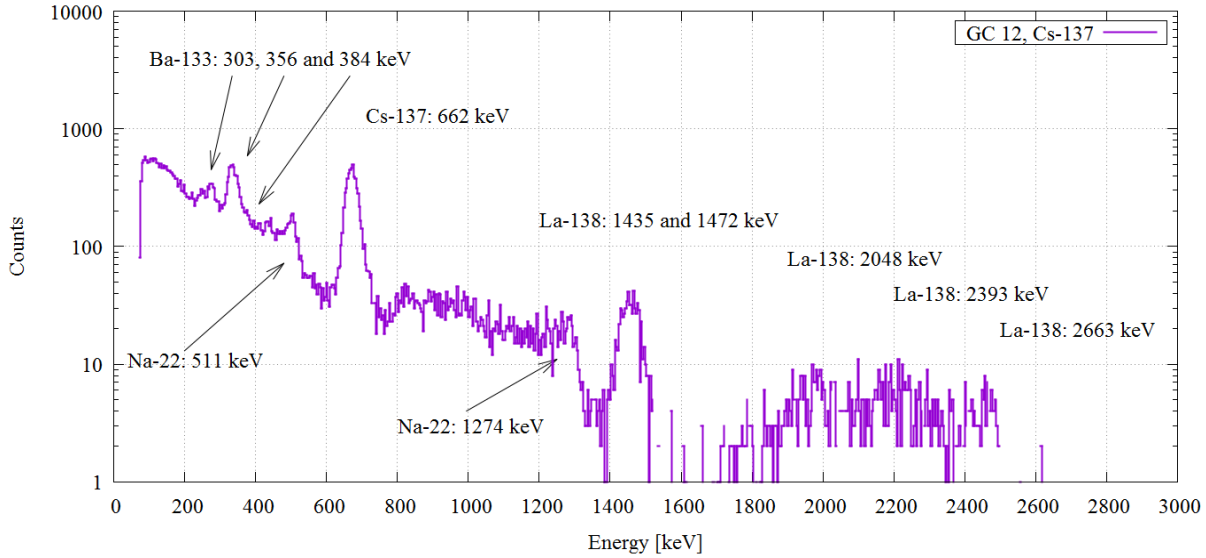

Fig. 53. Gamma spectrum in GC channel 12.

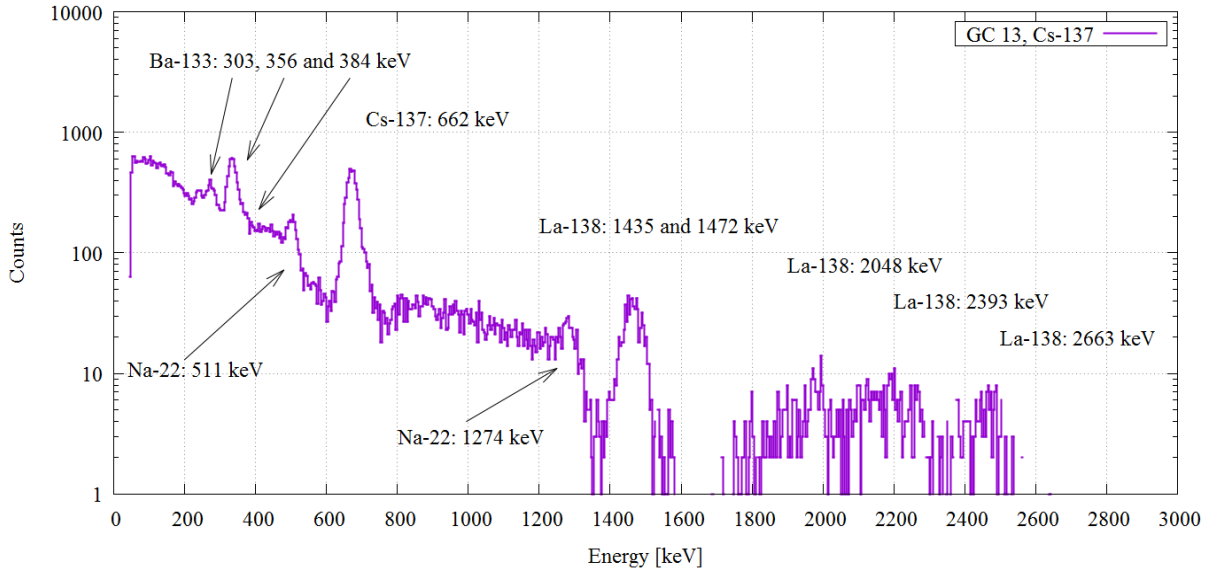

Fig. 54. Gamma spectrum in GC channel 13.

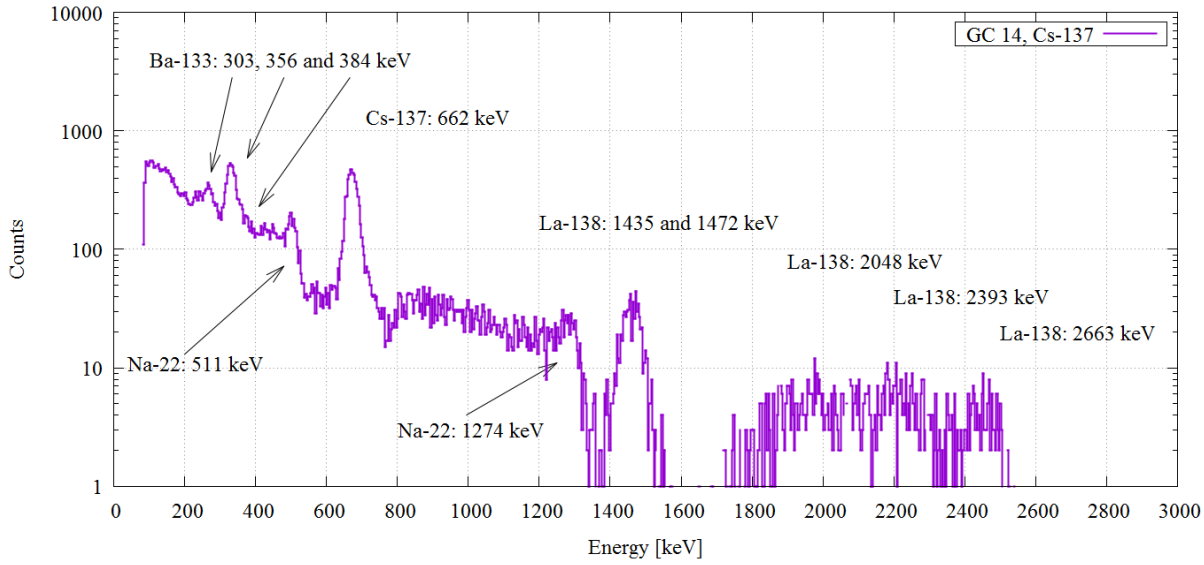

Fig. 55. Gamma spectrum in GC channel 14.

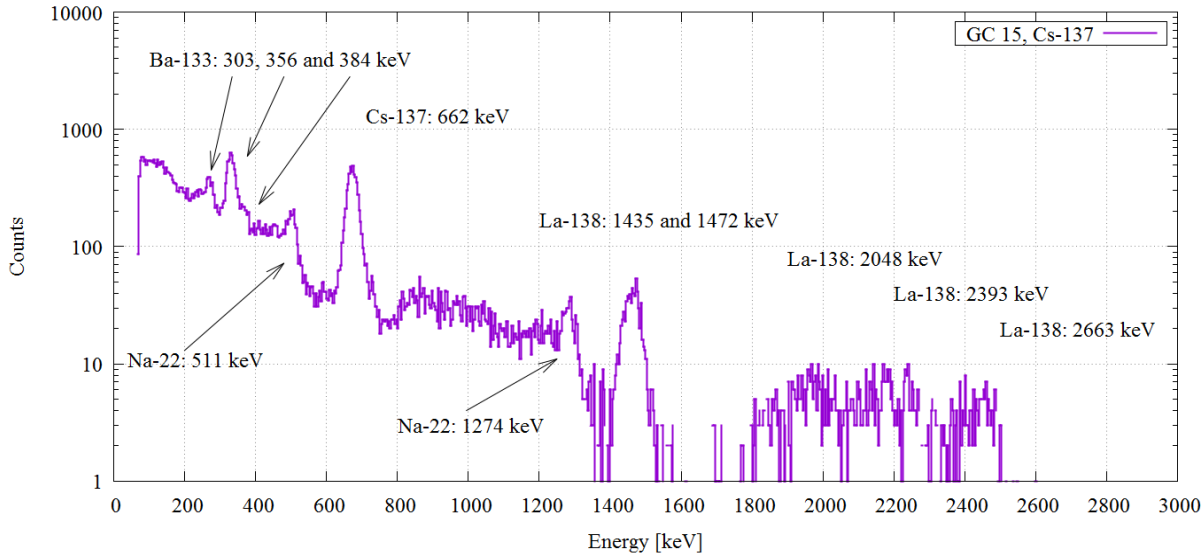

Fig. 56. Gamma spectrum in GC channel 15.

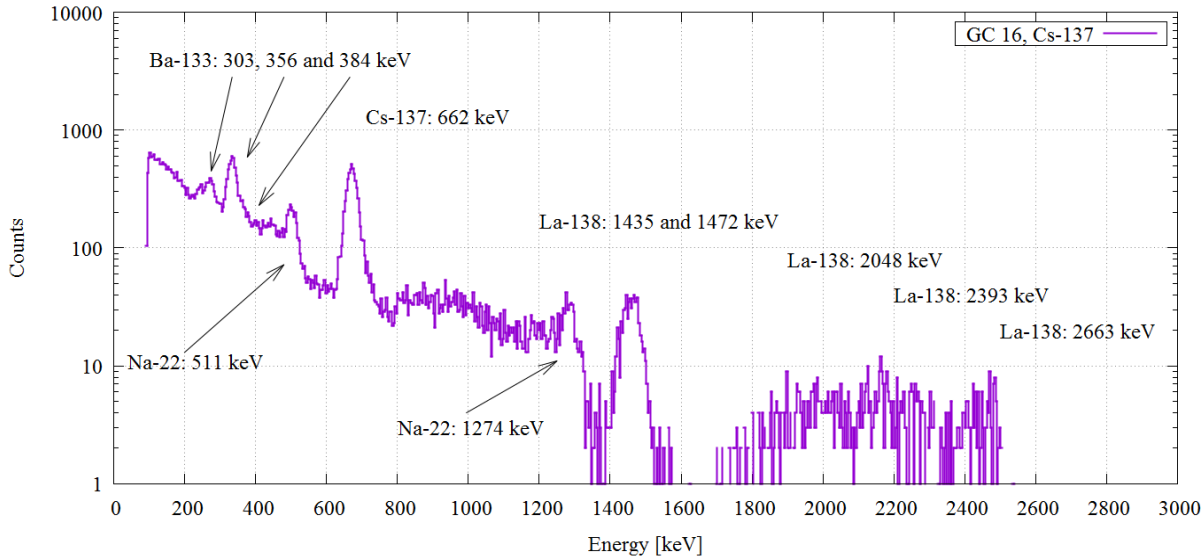

Fig. 57. Gamma spectrum in GC channel 16.

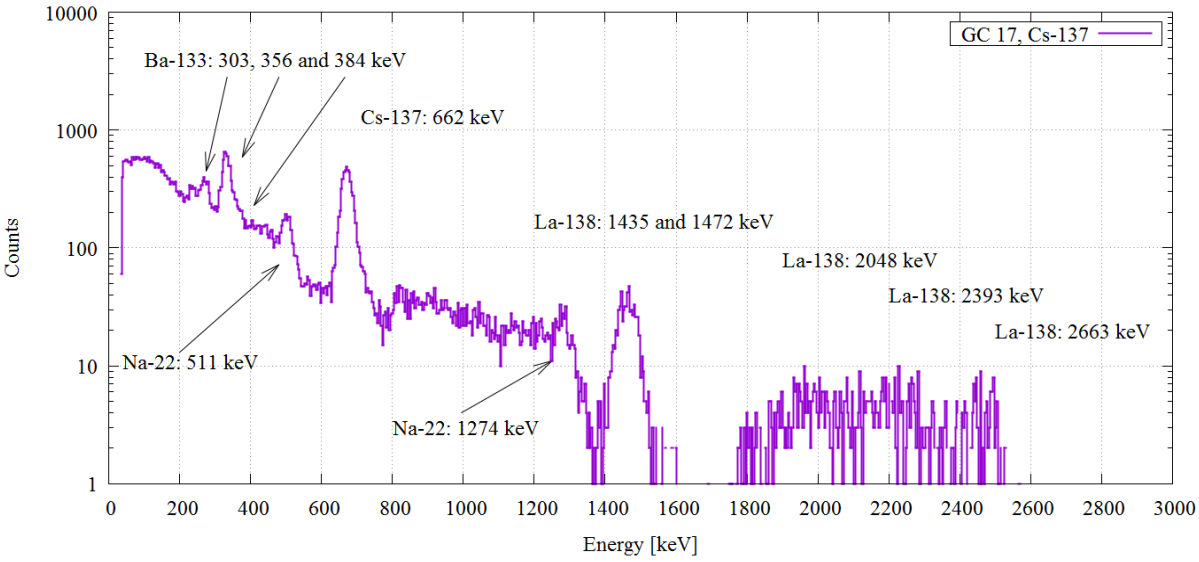

Fig. 58. Gamma spectrum in GC channel 17.

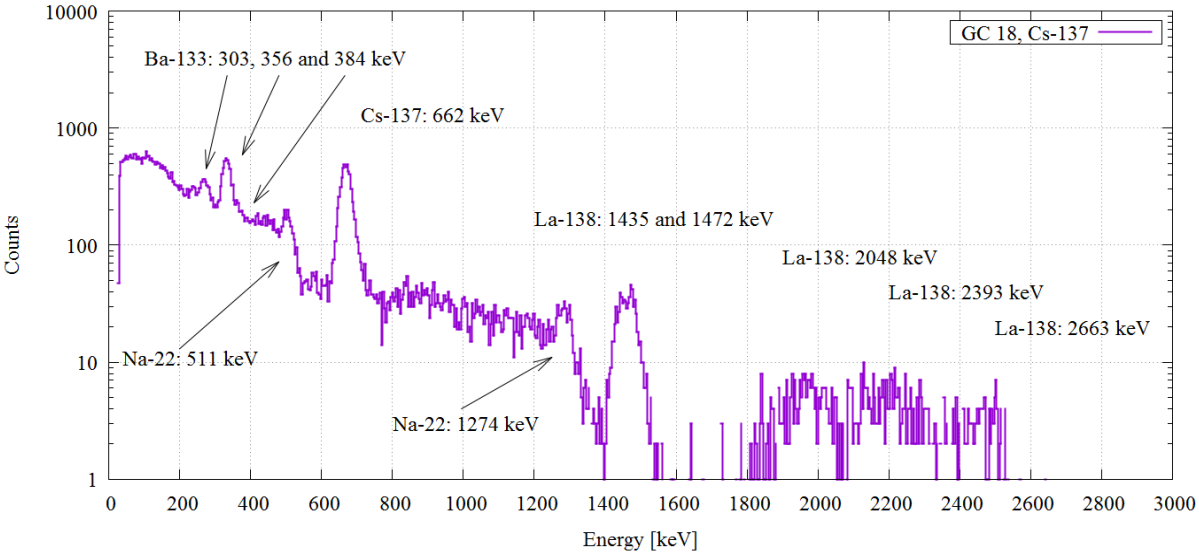

Fig. 59. Gamma spectrum in GC channel 18.

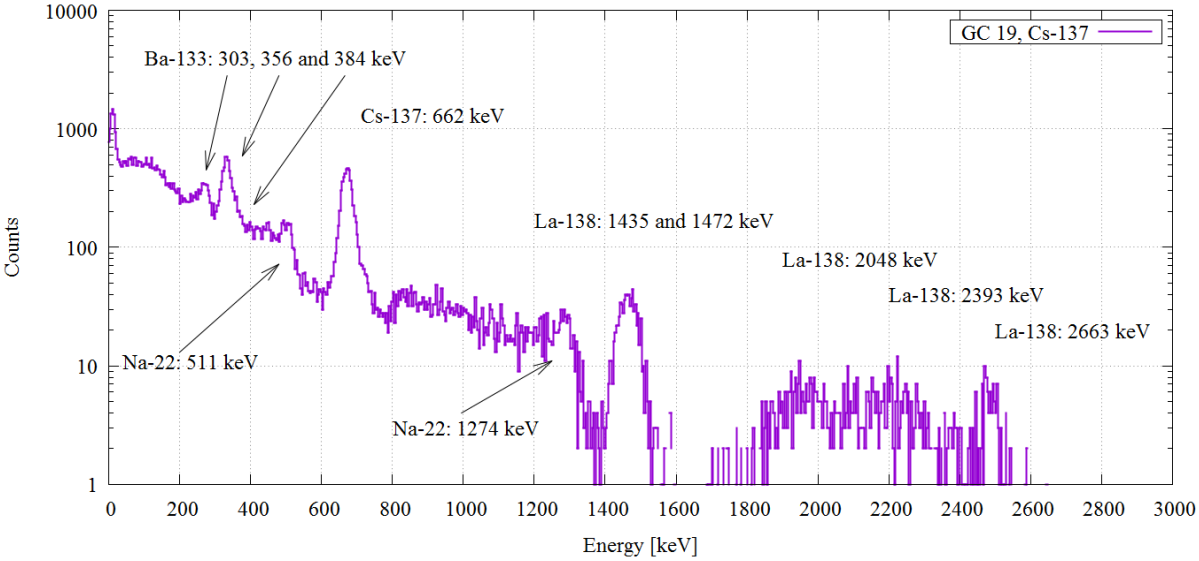

Fig. 60. Gamma spectrum in GC channel 19.

The report was prepared by

Andrzej Brosławski, Stefan Korolczuk and Arkadiusz Urban.

This scientific work was partly supported by Polish Ministry of Science and Higher Education within the framework of the scientific financial resources in the years 2015-2018 allocated for the realization of the international co-financed project.
This work has been carried out within the framework of the EUROfusion Consortium and has received funding from the Euratom research and training program 2014 - 2018 under grant agreement No 633053. The views and opinions expressed herein do not necessarily reflect those of the European Commission.